METHODS OF TREATING INFLAMMATORY SKIN DISEASES

The application claims priority to International Application No. PCT/US00/14142, filed on May 23, 2000, which claims priority to U.S. Provisional Application No. 60/138,133, filed on June 8, 1999. Throughout this application various publications are referenced. The disclosures of these publications in their entireties are hereby incorporated by reference into this application.

10

5

INTRODUCTION

The field of this invention is modified polypeptides with improved pharmacokinetics. Specifically, the field of this invention relates to Flt1 receptor polypeptides that have been modified in such a way as to improve their pharmacokinetic profile. The field of this invention also relates to methods of making and using the modified polypeptides including but not limited to using the modified polypeptides to decrease or inhibit plasma leakage and/or vascular permeability in a mammal and to treating various diseases in which plasma leakage and/or vascular permeability occurs, such as inflammatory skin diseases including, for example, psoriasis.

BACKGROUND

The ability of polypeptide ligands to bind to cells and thereby elicit a phenotypic response such as cell growth, survival, cell product secretion, or differentiation is often mediated through transmembrane receptors on the cells. The extracellular domain of such receptors (i.e.

EJJ125550J8802

25

5

10

that portion of the receptor that is displayed on the surface of the cell) is generally the most distinctive portion of the molecule, as it provides the protein with its ligand binding characteristic. Binding of a ligand to the extracellular domain generally results in signal transduction which transmits a biological signal to intracellular targets. signal transduction acts via a catalytic intracellular domain. The particular array of sequence motifs of this catalytic intracellular domain determines its access to potential kinase substrates (Mohammadi, et al.,1990, Mol. Cell. Biol. 11:5068-5078; Fantl, et al., 1992, Cell 69:413-413). Examples of receptors that transduce signals via catalytic intracellular domains include the receptor tyrosine kinases (RTKs) such as the Trk family of receptors which are generally limited to cells of the nervous system, the cytokine family of receptors including the tripartate CNTF receptor complex (Stahl & Yancopoulos, 1994, J. Neurobio. 25:1454-1466) which is also generally limited to the cells of the nervous system, G-protein coupled receptors such as the β_2 -adrenergic receptor found on, for instance, cardiac muscle cells, and the multimeric IgE high affinity receptor FcERI which is localized, for the most part, on mast cells and basophils (Sutton & Gould, 1993, Nature <u>366</u>:421-428).

All receptors identified so far appear to undergo dimerization, multimerization, or some related conformational change following ligand binding (Schlessinger, J., 1988, Trend Biochem. Sci. 13:443-447; Ullrich & Schlessinger, 1990, Cell 61:203-212; Schlessinger & Ullrich, 1992, Neuron 9:383-391) and molecular interactions between dimerizing intracellular domains lead to activation of catalytic function. In some instances, such as platelet-derived growth factor

25

5

(PDGF), the ligand is a dimer that binds two receptor molecules (Hart, et al., 1988, Science, 240:1529-1531; Heldin, 1989, J. Biol. Chem. 264:8905-8912) while, for example, in the case of epidermal growth factor (EGF), the ligand is a monomer (Weber, et al., 1984, J. Biol. Chem. 259:14631-14636). In the case of the FcεRI receptor, the ligand, IgE, exists bound to FcεRI in a monomeric fashion and only becomes activated when antigen binds to the IgE/FcεRI complex and cross-links adjacent IgE molecules (Sutton & Gould, 1993, Nature 366:421-428).

Often, the tissue distribution of a particular receptor within higher organisms provides insight into the biological function of the receptor. The RTKs for some growth and differentiation factors, such as fibroblast growth factor (FGF), are widely expressed and therefore appear to play some general role in tissue growth and maintenance. Members of the Trk RTK family (Glass & Yancopoulos, 1993, Trends in Cell Biol. 3:262-268) of receptors are more generally limited to cells of the nervous system, and the Nerve Growth Factor family consisting of nerve growth factor (NGF), brain-derived neurotrophic factor (BDNF), neurotrophin-3 (NT-3) and neurotrophin-4/5 (NT-4/5), which bind the Trk RTK family receptors, promote the differentiation of diverse groups of neurons in the brain and periphery (Lindsay, R. M, 1993, in Neurotrophic Factors, S.E. Loughlin & J.H. Fallon, eds., pp. 257-284, San Diego, CA, Academic Press). FcεRI is localized to a very limited number of types of cells such as mast cells and basophils. Mast cells derive from bone marrow pluripotent hematopoietic stem cell lineage, but complete their maturation in the tissue following migration from the blood stream (See Janeway & Travers, 1996, in Immunobiology, 2d. Edition, M. Robertson & E. Lawrence, eds., pp. 1:3-1:4, Current Biology

25

5

10

Ltd., London, UK, Publisher) and are involved in the allergic response.

Many studies have demonstrated that the extracellular domain of a receptor provides the specific ligand binding characteristic.

Furthermore, the cellular environment in which a receptor is expressed may influence the biological response exhibited upon binding of a ligand to the receptor. For example, when a neuronal cell expressing a Trk receptor is exposed to a neurotrophin which binds to that receptor, neuronal survival and differentiation results. When the same receptor is expressed by a fibroblast, exposure to the neurotrophin results in proliferation of the fibroblast (Glass, et al., 1991, Cell <u>66</u>:405-413).

A class of cell-derived dimeric mitogens with selectivity for vascular endothelial cells has been identified and designated vascular endothelial cell growth factor (VEGF). VEGF has been purified from conditioned growth media of rat glioma cells [Conn et al., (1990), Proc. Natl. Acad. Sci. U.S.A., 87. pp 2628-2632]; and conditioned growth media of bovine pituitary follicle stellate cells [Ferrara and Henzel, (1989), Biochem. Biophys. Res. Comm., 161, pp. 851-858; Gozpadorowicz et al., (1989), Proc. Natl. Acad. Sci. U.S.A., 86, pp. 7311-7315] and conditioned growth medium from human U937 cells [Connolly, D. T. et al. (1989), Science, 246, pp. 1309-1312]. VEGF is a dimer with an apparent molecular mass of about 46 kDa with each subunit having an apparent molecular mass of about 23 kDa. VEGF has some structural similarities to platelet derived growth factor (PDGF), which is a mitogen for connective tissue cells but not mitogenic for vascular endothelial cells from large vessels.

The membrane-bound tyrosine kinase receptor, known as Flt, was shown to be a VEGF receptor [DeVries, C. et al., (1992), Science, 255, pp.989-991]. The Flt receptor specifically binds VEGF which induces mitogenesis. Another form of the VEGF receptor, designated KDR, is also known to bind VEGF and induce mitogenesis. The partial cDNA sequence and nearly full length protein sequence of KDR is known as well [Terman, B. I. et al., (1991) Oncogene 6, pp. 1677-1683; Terman, B. I. et al., (1992) Biochem. Biophys. Res. Comm. 187, pp. 1579-1586].

Persistent angiogenesis may cause or exacerbate certain diseases such as psoriasis, rheumatoid arthritis, hemangiomas, angiofibromas, diabetic retinopathy and neovascular glaucoma. An inhibitor of VEGF activity would be useful as a treatment for such diseases and other VEGF-induced pathological angiogenesis and vascular permeability conditions, such as tumor vascularization. The present invention relates to a VEGF inhibitor that is based on the VEGF receptor Flt1.

Plasma leakage, a key component of inflammation, occurs in a distinct subset of microvessels. In particular, in most organs plasma leakage occurs specifically in the venules. Unlike arterioles and capillaries, venules become leaky in response to numerous inflammatory mediators including histamine, bradykinin, and serotonin. One characteristic of inflammation is the plasma leakage that results from intercellular gaps that form in the endothelium of venules. Most experimental models of inflammation indicate that these intercellular gaps occur between the endothelial cells of postcapillary and collecting venules (Baluk, P., et al., Am. J. Pathol. 1998 152:1463-76). It has been shown that certain lectins may be used to reveal features of focal sites of

25

plasma leakage, endothelial gaps, and finger-like processes at endothelial cell borders in inflamed venules (Thurston, G., et al., Am. J. Physiol, 1996, 271: H2547-62). In particular, plant lectins have been used to visualize morphological changes at endothelial cell borders in inflamed venules of, for example, the rat trachea. Lectins, such as conconavalin A and ricin, that bind focally to inflamed venules reveal regions of the subendothelial vessel wall exposed by gaps that correspond to sites of plasma leakage (Thurston, G., et al., Am J Physiol, 1996, 271: H2547-62).

10

5

The properties of the microvessels are dynamic. Chronic inflammatory diseases, for example, are associated with microvascular remodeling, including angiogenesis and microvessel enlargement. Microvessels can also remodel by acquiring abnormal phenotypic properties. In a murine model of chronic airway inflammation, airway capillaries acquire properties of venules, including widened vessel diameter, increased immunoreactivity for von Willebrand factor, and increased immunoreactivity for P-selectin. In addition, these remodeled vessels leak in response to inflammatory mediators, whereas vessels in the same position in the airways of normal mice do not.

Certain substances have been shown to decrease or inhibit vascular permeability and/or plasma leakage. For example, mystixins are synthetic polypeptides that have been reported to inhibit plasma leakage without blocking endothelial gap formation (Baluk, P., et al., J. Pharmacol. Exp. Ther., 1998, 284: 693-9). Also, the beta 2-adrenergic receptor agonist formoterol reduces microvascular leakage by

inhibiting endothelial gap formation (Baluk, P. and McDonald, D.M., Am. J. Physiol., 1994, 266:L461-8).

The angiopoietins and members of the vascular endothelial growth factor (VEGF) family are the only growth factors thought to be largely specific for vascular endothelial cells. Targeted gene inactivation studies in mice have shown that VEGF is necessary for the early stages of vascular development and that Ang-1 is required for later stages of vascular remodeling.

10

US Patent No. 6,011,003, issued January 4, 2000, in the name of Metris Therapeutics Limited, discloses an altered, soluble form of FLT polypeptide being capable of binding to VEGF and thereby exerting an inhibitory effect thereon, the polypeptide comprising five or fewer complete immunoglobulin domains.

US Patent No. 5,712,380, issued January 27, 1998 and assigned to Merck & Co., discloses vascular endothelial cell growth factor (VEGF) inhibitors that are naturally occurring or recombinantly engineered soluble forms with or without a C-terminal transmembrane region of the receptor for VEGF.

25

Also assigned to Merck & Co. is PCT Publication No. WO 98/13071, published April 2, 1998, which discloses gene therapy methodology for inhibition of primary tumor growth and metastasis by gene transfer of a nucleotide sequence encoding a soluble receptor protein which binds to VEGF.

25

5

PCT Publication No. WO 97/44453, published November 27, 1997, in the name of Genentech, Inc., discloses novel chimeric VEGF receptor proteins comprising amino acid sequences derived from the vascular endothelial growth factor (VEGF) receptors Flt1 and KDR, including the murine homologue to the human KDR receptor FLK1, wherein said chimeric VEGF receptor proteins bind to VEGF and antagonize the endothelial cell proliferative and angiogenic activity thereof.

PCT Publication No. WO 97/13787, published April 17, 1997, in the name of Toa Gosei Co., LTD., discloses a low molecular weight VEGF inhibitor usable in the treatment of diseases accompanied by neovascularization such as solid tumors. A polypeptide containing the first immunoglobulin-like domain and the second immunoglobulin-like domain in the extracellular region of a VEGF receptor FLT but not containing the sixth immunoglobulin-like domain and the seventh immunoglobulin-like domain thereof shows a VEGF inhibitory activity.

Sharifi, J. et al., 1998, The Quarterly Jour. of Nucl. Med. 42:242-249, disclose that because monoclonal antibodies (MAbs) are basic, positively charged proteins, and mammalian cells are negatively charged, the electrostatic interactions between the two can create higher levels of background binding resulting in low tumor to normal organ ratios. To overcome this effect, the investigators attempted to improve MAb clearance by using various methods such as secondary agents as well as chemical and charge modifications of the MAb itself.

Jensen-Pippo, et al., 1996, Pharmaceutical Research 13:102-107, disclose that pegylation of a therapeutic protein, recombinant human

granulocyte colony stimulating factor (PEG-G-CSF), results in an increase in stability and in retention of in vivo bioactivity when administered by the intraduodenal route.

Tsutsumi, et al., 1997, Thromb Haemost. 77:168-73, disclose 5 experiments wherein the in vivo thrombopoietic activity of polyethylene glycol-modified interleukin-6 (MPEG-IL-6), in which 54% of the 14 lysine amino groups of IL-6 were coupled with PEG, was compared to that of native IL-6.

10

Yang, et al., 1995, Cancer 76:687-94, disclose that conjugation of polyethylene glycol to recombinant human interleukin-2 (IL-2) results in a compound, polyethylene glycol-modified IL-2 (PEG-IL-2) that retains the in vitro and in vivo activity of IL-2, but exhibits a markedly prolonged circulating half-life.

R. Duncan and F. Spreafico, Clin. Pharmacokinet. 27: 290-306, 296 (1994) review efforts to improve the plasma half-life of asparaginase

by conjugating polyethylene glycol.

20

25

PCT International Publication No. WO 99/03996 published January 28, 1999 in the name of Regeneron Pharmaceuticals, Inc. and The Regents of The University of California describes modified human noggin polypeptides having deletions of regions of basic amino acids. The modified human noggin polypeptides are described as retaining biological activity while having reduced affinity for heparin and superior pharmacokinetics in animal sera as compared to the unmodified human noggin.

SUMMARY OF THE INVENTION

The present invention is directed to VEGF antagonists with improved pharmacokinetic properties. A preferred embodiment is an isolated nucleic acid molecule encoding a fusion polypeptide capable of binding a VEGF polypeptide comprising (a) a nucleotide sequence encoding a VEGF receptor component operatively linked to (b) a nucleotide sequence encoding a multimerizing component, wherein the VEGF receptor component is the only VEGF receptor component of the fusion polypeptide and wherein the nucleotide sequence of (a) consists essentially of a nucleotide sequence encoding the amino acid sequence of Ig domain 2 of the extracellular domain of a first VEGF receptor and a nucleotide sequence encoding the amino acid sequence of Ig domain 3 of the extracellular domain of a second VEGF receptor.

In a further embodiment, the isolated nucleic acid of the first VEGF receptor is Flt1.

In a further embodiment, the isolated nucleic acid of the second VEGF receptor is Flk1.

In yet another embodiment, the isolated nucleic acid of the second VEGF receptor is Flt4.

25

In another preferred embodiment, the nucleotide sequence encoding Ig domain 2 of the extracellular domain of the first VEGF receptor is

5

upstream of the nucleotide sequence encoding Ig domain 3 of the extracellular domain of the second VEGF receptor.

In still another preferred embodiment, the nucleotide sequence encoding Ig domain 2 of the extracellular domain of the first VEGF receptor is downstream of the nucleotide sequence encoding Ig domain 3 of the extracellular domain of the second VEGF receptor.

In a preferred embodiment of the invention, the multimerizing component comprises an immunoglobulin domain.

In another embodiment, the immunoglobulin domain is selected from the group consisting of the Fc domain of IgG, the heavy chain of IgG, and the light chain of IgG.

Preferred embodiments include an isolated nucleic acid molecule comprising a nucleotide sequence encoding a modified Flt1 receptor fusion polypeptide, wherein the coding region of the nucleic acid molecule consists of a nucleotide sequence selected from the group consisting of

- (a) the nucleotide sequence set forth in Figure 13A-13D;
- (b) the nucleotide sequence set forth in Figure 14A-14C;
- (c) the nucleotide sequence set forth in Figure 15A-15C;
- (d) the nucleotide sequence set forth in Figure 16A-16D;
- 25 (e) the nucleotide sequence set forth in Figure 21A-21C;
 - (f) the nucleotide sequence set forth in Figure 22A-22C;
 - (g) the nucleotide sequence set forth in Figure 24A-24C; and
 - (h) a nucleotide sequence which, as a result of the degeneracy of the

genetic code, differs from the nucleotide sequence of (a), (b), (c), (d), (e), (f), or (g) and which encodes a fusion polypeptide molecule having the biological activity of the modified Flt1 receptor fusion polypeptide.

In a further embodiment of the invention, a fusion polypeptide is encoded by the isolated nucleic acid molecules described above.

A preferred embodiment is a composition capable of binding a VEGF molecule to form a nonfunctional complex comprising a multimer of the fusion polypeptide.

Also preferred is a composition wherein the multimer is a dimer.

In yet another embodiment, the composition is in a carrier.

Another embodiment is a vector which comprises the nucleic acid molecules described above, including an expression vector comprising a the nucleic acid molecules described wherein the nucleic acid molecule is operatively linked to an expression control sequence.

20

25

Other included embodiments are a host-vector system for the production of a fusion polypeptide which comprises the expression vector, in a suitable host cell; the host-vector system wherein the suitable host cell is a bacterial cell, yeast cell, insect cell, or mammalian cell; the host-vector system wherein the suitable host cell is <u>E. Coli</u>; the host-vector system wherein the suitable host cell is a COS cell; the host-vector system wherein the suitable host cell is a CHO cell.

5

Another embodiment of the invention is a method of producing a fusion polypeptide which comprises growing cells of the host-vector system under conditions permitting production of the fusion polypeptide and recovering the fusion polypeptide so produced.

Additional embodiments include a fusion polypeptide encoded by the nucleic acid sequence set forth in Figure 10A-10D or Figure 24A-24C, which has been modified by acetylation or pegylation wherein the acetylation is accomplished with at least about a 100 fold molar excess of acetylation reagent or wherein acetylation is accomplished with a molar excess of acetylation reagent ranging from at least about a 10 fold molar excess to about a 100 fold molar excess or wherein the pegylation is 10K or 20K PEG.

A preferred embodiment includes a method of decreasing or inhibiting plasma leakage in a mammal comprising administering to the mammal the fusion polypeptide described above, including embodiments wherein the mammal is a human, the fusion polypeptide is acetylated or the fusion polypeptide is pegylated.

A further embodiments is a fusion polypeptide which specifically binds the VEGF receptor ligand VEGF.

A preferred embodiment of the invention is a method of blocking blood vessel growth in a human comprising administering an effective amount of the fusion polypeptide described above.

25

10

Also preferred is a method of inhibiting VEGF receptor ligand activity in a mammal comprising administering to the mammal an effective amount of the fusion polypeptide described above.

5 Preferred embodiments of these methods are wherein the mammal is a human.

attenuation or prevention of tumor growth in a human; attenuation or prevention of edema in a human, especially wherein the edema is brain edema; attenuation or prevention of ascites formation in a human, especially wherein the ascites is ovarian cancer-associated ascites.

Preferred embodiments of the invention include a fusion polypeptide capable of binding a VEGF polypeptide comprising (a) a VEGF receptor component operatively linked to (b) a multimerizing component, wherein the VEGF receptor component is the only VEGF receptor component in the fusion polypeptide and consists essentially of the amino acid sequence of Ig domain 2 of the extracellular domain of a first VEGF receptor and the amino acid sequence of Ig domain 3 of the extracellular domain of a second VEGF receptor.

In a further embodiment of the fusion polypeptide, the first VEGF receptor is Flt1.

In yet a further embodiment of the fusion polypeptide, the second VEGF receptor is Flk1.

25

5

10

Still another embodiment of the fusion polypeptide is one in which the second VEGF receptor is Flt4.

Preferred embodiments include a fusion polypeptide wherein amino acid sequence of Ig domain 2 of the extracellular domain of the first VEGF receptor is upstream of the amino acid sequence of Ig domain 3 of the extracellular domain of the second VEGF receptor and a fusion polypeptide wherein the amino acid sequence of Ig domain 2 of the extracellular domain of the first VEGF receptor is downstream of the amino acid sequence of Ig domain 3 of the extracellular domain of the second VEGF receptor.

In yet another embodiment, the fusion polypeptide multimerizing component comprises an immunoglobulin domain including an embodiment wherein the immunoglobulin domain is selected from the group consisting of the Fc domain of IgG, the heavy chain of IgG, and the light chain of IgG.

Preferred embodiments include a fusion polypeptide comprising an amino acid sequence of a modified Flt1 receptor, wherein the amino acid sequence selected from the group consisting of (a) the amino acid sequence set forth in Figure 13A-13D; (b) the amino acid sequence set forth in Figure 14A-14C; (c) the amino acid sequence set forth in Figure 15A-15C; (d) the amino acid sequence set forth in Figure 16A-16D; (e) the amino acid sequence set forth in Figure 21A-21C; (f) the amino acid sequence set forth in Figure 22A-22C; and (g) the amino acid sequence set forth in Figure 24A-24C.

25

Another preferred embodiment is a method of decreasing or inhibiting plasma leakage in a mammal comprising administering to the mammal the fusion polypeptide described above.

An alternative preferred embodiment is a method of inhibiting VEGF receptor ligand activity in a mammal comprising administering to the mammal an effective amount of the fusion polypeptide described above.

One embodiment of the invention is a method of treating psoriasis in a mammal comprising administering a VEGF antagonist to the mammal, and in particular administering VEGFR1R2-Fc Δ C1(a) to the mammal.

Another preferred embodiment is a method of treating psoriasis in a human comprising administering a VEGF antagonist to the human, and in particular, administering VEGFR1R2-Fc Δ C1(a) to the human.

Yet another embodiment is a method of reducing the severity of a psoriatic lesion in a mammal comprising administering a VEGF antagonist to the mammal, and in particular, administering VEGFR1R2- $Fc\Delta C1(a)$ to the mammal.

Also preferred is a method of reducing the severity of a psoriatic lesion in a human comprising administering a VEGF antagonist to the human, and in particular, administering VEGFR1R2-Fc∆C1(a) to the human.

Still another preferred embodiment is a method of minimizing the extent of hyperproliferation of keratinocytes associated with psoriasis

in a human comprising administering a VEGF antagonist to the human and in particular, administering VEGFR1R2-Fc\(\Delta\)C1(a) to the human.

Also preferred is a method of reducing the extent of hyperproliferated keratinocytes associated with psoriasis in a human comprising administering a VEGF antagonist to the human, and in particular, administering VEGFR1R2-FcΔC1(a) to the human.

5

10

then then the their field

<u>1</u> 5

An additional preferred embodiment of the invention is a method of minimizing the extent of epidermal hyperplasia associated with psoriasis in a human comprising administering a VEGF antagonist to the human, and in particular, administering VEGFR1R2-Fc Δ C1(a) to the human.

One preferred embodiment is a method of reversing epidermal hyperplasia associated with psoriasis in a human comprising administering a VEGF antagonist to the human, and in particular, administering VEGFR1R2-Fc Δ C1(a) to the human.

20 Still other preferred embodiments include methods of treating parakeratosis associated with psoriasis in a human comprising administering a VEGF antagonist to the human, in particular administering VEGFR1R2-FcΔC1(a) to the human and treating microabcess associated with psoriasis in a human comprising administering a VEGF antagonist to the human, in particular administering VEGFR1R2-FcΔC1(a) to the human.

Also contemplated is the preferred method of decreasing reteridges associated with psoriasis in a human comprising administering a VEGF

10

antagonist to the human, and in particular, administering VEGFR1R2-Fc Δ C1(a) to the human.

An additional contemplated embodiment is a method of treating inflammatory skin disease in a human comprising administering to the human VEGFR1R2-Fc\(\Delta\)C1(a).

Yet a further embodiment is a method of preventing the infiltration of lymphocytes from the dermis into the epidermis of a human comprising administering VEGFR1R2-Fc Δ C1(a) to the human.

In preferred embodiments of the invention the administration is topical administration, subcutaneous administration, or perhaps intramuscular, intranasal, intrathecal, intraarterial, intravenous, transvaginal, transdermal, or transanal administration.

Preferred embodiments include the use of a VEGF antagonist to treat psoriasis in a mammal and in particular to treat psoriasis in a human.

20 A further embodiment is the use of VEGFR1R2-Fc∆C1(a) to treat psoriasis in a human.

One embodiment of the invention is a method of treating psoriasis in a mammal comprising administering a VEGF antagonist to the mammal, and in particular administering VEGFR1R2-Fc Δ C1(a) to the mammal.

Another preferred embodiment is a method of treating psoriasis in a human comprising administering a VEGF antagonist to the human, and in particular, administering VEGFR1R2-Fc Δ C1(a) to the human.

Yet another embodiment is a method of reducing the severity of a psoriatic lesion in a mammal comprising administering a VEGF antagonist to the mammal, and in particular, administering VEGFR1R2- $Fc\Delta C1(a)$ to the mammal.

5

Also preferred is a method of reducing the severity of a psoriatic lesion in a human comprising administering a VEGF antagonist to the human, and in particular, administering VEGFR1R2-Fc∆C1(a) to the human.

10

Still another preferred embodiment is a method of minimizing the extent of hyperproliferation of keratinocytes associated with psoriasis in a human comprising administering a VEGF antagonist to the human and in particular, administering VEGFR1R2-Fc∆C1(a) to the human.

1 5

Also preferred is a method of reducing the extent of hyperproliferated keratinocytes associated with psoriasis in a human comprising administering a VEGF antagonist to the human, and in particular, administering VEGFR1R2-Fc∆C1(a) to the human.

An additional preferred embodiment of the invention is a method of minimizing the extent of epidermal hyperplasia associated with psoriasis in a human comprising administering a VEGF antagonist to the human, and in particular, administering VEGFR1R2-Fc∆C1(a) to the human.

25

One preferred embodiment is a method of reversing epidermal hyperplasia associated with psoriasis in a human comprising

5

administering a VEGF antagonist to the human, and in particular, administering VEGFR1R2-Fc\(\Delta\)C1(a) to the human.

Still other preferred embodiments include methods of treating parakeratosis associated with psoriasis in a human comprising administering a VEGF antagonist to the human, in particular administering VEGFR1R2-Fc Δ C1(a) to the human and treating microabcess associated with psoriasis in a human comprising administering a VEGF antagonist to the human, in particular administering VEGFR1R2-Fc Δ C1(a) to the human.

Also contemplated is the preferred method of decreasing reteridges associated with psoriasis in a human comprising administering a VEGF antagonist to the human, and in particular, administering VEGFR1R2- $Fc\Delta C1(a)$ to the human.

An additional contemplated embodiment is a method of treating inflammatory skin disease in a human comprising administering to the human VEGFR1R2-Fc Δ C1(a).

Yet a further embodiment is a method of preventing the infiltration of lymphocytes from the dermis into the epidermis of a human comprising administering VEGFR1R2-Fc Δ C1(a) to the human.

A further embodiment of the invention is a method of enhancing wound healing in a human comprising administering a VEGF antagonist to the human.

5

Another preferred embodiment is a method of enhancing wound healing in a human comprising administering VEGFR1R2-Fc\(\Delta\)C1(a) to the human.

In preferred embodiments of the invention the administration is topical administration, subcutaneous administration, or perhaps intramuscular, intranasal, intrathecal, intraarterial, intravenous, transvaginal, transdermal, or transanal administration.

Preferred embodiments include the use of a VEGF antagonist to treat 10 psoriasis in a mammal and in particular to treat psoriasis in a human.

A further embodiment is the use of VEGFR1R2-Fc Δ C1(a) to treat psoriasis in a human.

BRIEF DESCRIPTION OF THE FIGURES

Figure 1. IEF gel analysis of unmodified and acetylated Flt1(1-3)-Fc proteins. Unmodified Flt1(1-3)-Fc protein is unable to enter the gel due to its >9.3 pl, whereas acetylated Flt1(1-3)-Fc is able to enter the gel and equilibrate at pl 5.2.

Figure 2. Binding of unmodified Flt1(1-3)-Fc and acetylated Flt1(1-3)-Fc proteins to Matrigel® coated plates. Unmodified Flt1(1-3)-Fc proteins binds extensive to extracellular matrix components in Matrigel®, whereas acetylated Flt1(1-3)-Fc does not bind.

Figure 3. Binding of unmodified Flt1(1-3)-Fc, acetylated Flt1(1-3)-Fc, and pegylated Flt1(1-3)-Fc in a Biacore-based assay. Acetylated (columns 13-16), pegylated (columns 17-20), and heparin-treated

Flt1(1-3)-Fc (columns 21-24) are each able to completely compete with the Biacore chip-bound Flt1(1-3)-Fc for VEGF binding as compared to control (columns 1-4) and irrelevant protein (columns 5-8). Unmodified Flt1(1-3)-Fc (columns 5-6) appears to only partially compete with Biacore chip-bound Flt1(1-3)-Fc for VEGF binding. However, washing the bound samples with 0.5M NaCl (columns 7-8) results in a binding profile similar to the modified forms of Flt1(1-3)-Fc, indicating that the unmodified protein is exhibiting non-specific binding to the chip that can be eliminated by the salt wash.

10

5

Figure 4. Binding of unmodified Flt1(1-3)-Fc, acetylated Flt1(1-3)-Fc, and pegylated Flt1(1-3)-Fc to VEGF in an ELISA-based assay. Both pegylated and acetylated Flt1(1-3)-Fc proteins bind to VEGF with affinities approaching that of unmodified Flt1(1-3)-Fc.

1 5

20

Figure 5. Pharmacokinetic profiles of unmodified Flt1(1-3)-Fc, acetylated Flt1(1-3)-Fc, and pegylated Flt1(1-3)-Fc. Balb/c mice (23-28g) were injected subcutaneously with 4mg/kg of unmodified, acetylated, or pegylated Flt1(1-3)-Fc. The mice were tail bled at 1, 2, 4, 6, 24 hours, 2 days, and 3 days after injection of protein and the sera were assayed in a standard ELISA-based assay designed to detect Flt1(1-3)-Fc protein. The T_{max} for all of the Flt1(1-3)-Fc proteins was between the 6 hour and 24 hour time points. The C_{max} for the different proteins was as follows: Unmodified: 0.06 μ g/ml - 0.15 μ g/ml; acetylated: 1.5 μ g/ml - 4.0 μ g/ml; and pegylated: approximately 5 μ g/ml.

25

25

5

Figure 6A-6B. IEF gel analysis of unmodified and step-acetylated Flt1(1-3)-Fc proteins. Unmodified Flt1(1-3)-Fc protein is unable to enter the gel due to its >9.3 pl, whereas most of the step-acetylated Flt1(1-3)-Fc samples (30-100 fold excess samples) were able to migrate into the gel and equilibrate at pls ranging between 4.55 - 8.43, depending on the degree of acetylation.

Figure 7. Binding of unmodified Flt1(1-3)-Fc and step-acetylated Flt1(1-3)-Fc proteins to Matrigel® coated plates. As with the irrelevant control protein, rTie2-Fc, step-acetylated Flt1(1-3)-Fc (20 and 30 fold excess samples) does not exhibit any binding to the Matrigel coated plate, whereas the non-acetylated Flt1(1-3)-Fc protein exhibits significant binding. The 10 fold excess sample shows reduced binding, but the degree of acetylation is not enough to completely block binding to extracellular matrix components.

Figure 8. Binding of unmodified Flt1(1-3)-Fc and step-acetylated Flt1(1-3)-Fc in a Biacore-based assay. At a sub-stoichiometric ratio $(0.5~\mu\text{g/ml})$ of either unmodified Flt1(1-3) or step-acetylated Flt1(1-3)-Fc vs. $0.2~\mu\text{g/ml}$ VEGF), there is not enough Flt1(1-3)-Fc (either unmodified or step-acetylated) in the solution to completely bind the VEGF. At $1.0~\mu\text{g/ml}$, which approximates a 1:1 stoichiometric ratio, the both unmodified and step-acetylated Flt1(1-3)-Fc are better able to compete for VEGF binding, but there is still insufficient Flt1(1-3)-Fc protein (either unmodified or step-acetylated) to completely saturate the available VEGF. However, at $5.0~\mu\text{g/ml}$, which is several times

greater than a 1:1 stoichiometric ratio, both the Flt1(1-3)-Fc and the step-acetylated Flt1(1-3)-Fc proteins are able to saturate the VEGF, regardless of the degree of acetylation.

Figure 9. Pharmacokinetic profiles of unmodified Flt1(1-3)-Fc and step-acetylated Flt1(1-3)-Fc. Balb/c mice (23-28g) were injected subcutaneously with 4mg/kg of unmodified or 10, 20, 40, 60 and 100 fold excess samples of step-acetylated Flt1(1-3)-Fc (3 mice for unmodified, 10, 20 and 40 fold excess samples and 2 mice for 60 and 100 fold excess samples). The mice were tail bled at 1, 2, 4, 6, 24 hours, 2 days and 3 days after injection. The sera were assayed in an ELISA-based assay designed to detect Flt1(1-3)-Fc. The T_{max} for all of the Flt1(1-3)-Fc proteins tested was at the 6 hour time point but the C_{max} was as follows: Unmodified Flt1(1-3)-Fc: 0.06μg/ml; 10 fold excess sample: - 0.7μg/ml, 20 fold excess sample - 2μg/ml, 40 fold excess sample - 4μg/ml, 60 fold excess sample - 2μg/ml, 100 fold excess sample - 1μg/ml.

Figure 10A-10D. Nucleic acid and deduced amino acid sequence of Flt1(1-3)-Fc.

Figure 11. Schematic diagram of the structure of Flt1.

Figure 12A and 12B. Hydrophilicity analysis of the amino acid sequences of Ig domain 2 and Ig domain 3 of Flt1.

Figure 13A-13D. Nucleic acid and deduced amino acid sequence of Mut1: Flt1(1-3 $_{\Delta B}$)-Fc.

20

25

Figure 14A-14 C. Nucleic acid and deduced amino acid sequence of Mut2: $Flt1(2-3_{AB})-Fc$.

Figure 15A-15C. Nucleic acid and deduced amino acid sequence of Mut3: Flt1(2-3)-Fc.

Figure 16A-16D. Nucleic acid and deduced amino acid sequence of Mut4: $Flt1(1-3_{R->N})$ -Fc.

Figure 17. Binding of unmodified Flt1(1-3)-Fc, basic region deletion mutant Flt1(1-3)-Fc, and Flt1(1-3)_{R->N} mutant proteins in a Biacorebased assay. At the sub-stoichiometric ratio (0.25 μ g/ml Flt1(1-3)-Fc of unmodified, acetylated or genetically modified samples vs. 01. μ g/ml VEGF), there is insufficient Flt1(1-3)-Fc protein to block binding of VEGF to the Flt1(1-3)-Fc immobilized on the Biacore chip. At 0.5 μ g/ml of unmodified, acetylated or genetically modified Flt1(1-3)-Fc proteins, the stoichiometric ratio approximates 1:1 and there is an increased ability to block VEGF binding to the Biacore chip. At 1.0 μ g/ml of unmodified, acetylated or genetically modified Flt1(1-3)-Fc proteins, which is approximately a 10:1 stoichiometric ratio, the FIt1(1-3)-Fc proteins are able to block binding of VEGF to the Biacore chip, but they are not equivalent. Unmodified, acetylated, and Mut1: Flt1(1-3 $_{\Delta B}$)-Fc are essentially equal in their ability to block VEGF binding, whereas Mut4: Flt1(1-3_{R->N})-Fc is somewhat less efficient at blocking binding.

Figure 18. Binding of unmodified Flt1(1-3)-Fc, Mut1: Flt1(1- $3_{\Delta B}$)-Fc, Mut2: Flt1(2- $3_{\Delta B}$)-Fc, and Flt1(2-3) mutant proteins to Matrigel® coated plates. Unmodified Flt1(1-3)-Fc protein binds avidly to these wells, the Mut3: Flt1(2-3)-Fc protein binds somewhat more weakly, the Mut1: Flt1(1- $3_{\Delta B}$)-Fc protein binds more weakly still, and the Mut2: Flt1(2- $3_{\Delta B}$)-Fc protein shows the best profile, binding more weakly than any of the other mutant proteins. The Mut4: Flt1(1- $3_{R->N}$)-Fc glycosylation mutant protein shows only marginal benefit on the Matrigel assay.

Figure 19. Binding of unmodified Flt1(1-3)-Fc, Mut1: Flt1(1-3 $_{\Delta B}$)-Fc, Mut2: Flt1(2-3 $_{\Delta B}$)-Fc, and Flt1(2-3) mutant proteins in an ELISA-based assay. At the concentrations tested, unmodified Flt1(1-3)-Fc, Mut1: Flt1(1-3 $_{\Delta B}$)-Fc, Mut2: Flt1(2-3 $_{\Delta B}$)-Fc, and Flt1(2-3) mutant proteins bind VEGF similarly.

Figure 20. Pharmacokinetic profiles of unmodified Flt1(1-3)-Fc, Mut1: Flt1(1-3 $_{\Delta B}$)-Fc, Mut2: Flt1(2-3 $_{\Delta B}$)-Fc, and Flt1(2-3) mutant proteins. the Cmax for these reagents was as follows: Unmodified Flt1(1-3)-Fc - 0.15 μ g/ml; 40 fold molar excess acetylated Flt1(1-3)-Fc - 1.5 μ g/ml; and Mut1: Flt1(1-3 $_{\Delta B}$)-Fc - 0.7 μ g/ml.

Figure 21A-21C. Nucleotide and deduced amino acid sequence of the modified Flt1 receptor termed Flt1D2.Flk1D3.Fc∆C1(a).

Figure 22A-22C. Nucleotide and deduced amino acid sequence of the modified Flt1 receptor termed Flt1D2.VEGFR3D3.Fc∆C1(a).

Figure 23. Extracellular Matrix (ECM) Assay. The results of this assay demonstrate that the Flt1D2.Flk1D3.FcΔC1(a) and Flt1D2.VEGFR3D3.FcΔC1(a) proteins are considerably less sticky to the ECM as compared to the Flt1(1-3)-Fc protein.

Figure 24A-24C. Nucleotide and deduced amino acid sequence of the modified Flt1 receptor termed VEGFR1R2-Fc Δ C1(a).

Figure 25A-25C. Phosphorylation assay. At a 1.5 molar excess of either Flt1(1-3)-Fc , Flt1(1-3)-Fc (A40) or transient

Flt1D2Flk1D3.FcΔC1(a) there is complete blockage of receptor stimulation by these three modified Flt1 receptors as compared to control media challenge. In contrast, transient

Flt1D2VEGFR3D3.FcΔC1(a) does not show significant blockage at this molar excess, as compared with VEGF positive control challenge.

Similar results are seen in Figure 25B, where the modified Flt receptors are in a 3-fold molar excess to VEGF165 ligand. In Figure 25C, where the modified Flt1 receptors are in a 6-fold molar excess to VEGF165 ligand, transient Flt1D2VEGFR3D3.FcΔC1(a) can now be shown to be partially blocking VEGF165-induced stimulation of cell-surface receptors.

20

Figure 26A-26B. Phosphorylation assay. Detection by Western blot of tyrosine phosphorylated VEGFR2(Flk1) by VEGF165 ligand stimulation shows that cell-surface receptors are not phosphorylated by challenge samples which have VEGF165 preincubated with 1 and 2 fold molar excess (Figure 26A) or 3 and 4 fold molar excess (Figure 26B) of either transient Flt1D2Flk1D3.FcΔC1(a), stable Flt1D2Flk1D3.FcΔC1(a), or transient VEGFR1R2-FcΔC1(a). At all modified Flt1 receptor concentrations tested there is complete binding of VEGF165 ligand during the preincubation, resulting in no detectable stimulation of cell-surface receptors by unbound VEGF165 as compared to control media challenge.

Figure 27. MG/R2 Cell proliferation assay. The following modified Flt receptors Flt1(1-3)-Fc, Flt1D2.Flk1D3.FcΔC1(a) and Flt1D2.VEGFR3D3.FcΔC1(a), plus an irrelevant receptor termed Tie2-Fc as a negative control, were titrated from 40nM to 20pM and incubated on the cells for 1hr at 37°C. Human recombinant VEGF165 in defined media was then added to all the wells at a concentration of 1.56nM. The negative control receptor Tie2-Fc does not block VEGF165-induced cell proliferation at any concentration whereas Flt1D2.Flk1D3.FcΔC1(a) blocks 1.56nM VEGF165 with a half maximal dose of 0.8nM. Flt1(1-3)-Fc and Flt1D2.VEGFR3D3.FcΔC1(a) are less effective in blocking VEGF165 in this assay with a half maximal dose of ~ 2nM. VEGF165 alone gives a reading of 1.2 absorbance units and the background is 0.38 absorbance units.

Figure 28. Biacore analysis of Binding Stoichiometry. Binding stoichiometry was calculated as a molar ratio of bound VEGF165 to the immobilized Flt1D2Flk1D3.FcΔC1(a) or VEGFR1R2-FcΔC1(a), using the conversion factor of 1000 RU equivalent to 1 ng/ml. The results indicated binding stoichiometry of one VEGF165 dimeric molecule per one Flt1D2Flk1D3.FcΔC1(a) or VEGFR1R2-FcΔC1(a) molecule.

Figure 29 and Figure 30. Size Exclusion Chromatography Stoichiometry. Flt1D2Flk1D3.FcΔC1(a) or VEGFR1R2-FcΔC1(a) at a concentration of 1nM (estimated to be 1000 times higher than the KD of the Flt1D2Flk1D3.FcΔC1(a) or VEGFR1R2-FcΔC1(a)/VEGF165 interaction) were mixed with varied concentrations of VEGF165. After incubation, concentrations of the free Flt1D2Flk1D3.FcΔC1(a) in solution were measured. The data shows that the addition of 1 nM VEGF165 into the Flt1D2Flk1D3.FcΔC1(a) solution completely blocks Flt1D2Flk1D3.FcΔC1(a) binding to the VEGF165 surface. This result suggested the binding stoichiometry of one VEGF165 molecule per one Flt1D2Flk1D3.FcΔC1(a) molecule.

Figure 31. Size Exclusion Chromatography (SEC) under native conditions. Peak #1 represents the Flt1D2Flk1D3.FcΔC1(a)/ VEGF165 complex and peak #2 represents unbound VEGF165. Fractions eluted between 1.1 and 1.2 ml were combined and guanidinium hydrochloride (GuHCl)was added to a final concentration 4.5M to dissociate the complex.

25

5

Figure 32. Size Exclusion Chromatography (SEC) under dissociative conditions. To separate the components of the receptor-ligand complex and to determine their molar ratio, 50μl of dissociated complex was loaded onto a Superose 12 PC 3.2/30 equilibrated in 6M GuHCl and eluted. Peak #1 represents Flt1D2Flk1D3.FcΔC1(a) and peak #2 represents VEGF165.

Figure 33, Figure 34 and Figure 35. Size Exclusion
Chromatography (SEC) with On-Line Light Scattering. Size exclusion
chromatography column with a MiniDawn on-line light scattering
detector (Wyatt Technology, Santa Barbara, California) and refractive
index (RI) detectors (Shimadzu, Kyoto, Japan) was used to determine
the molecular weight (MW) of the receptor-ligand complex. As shown in
Figure 33, the elution profile shows two peaks. Peak #1 represents the
receptor-ligand complex and peak #2 represents the unbound VEGF165.
MW was calculated from LS and RI signals. The same procedure was
used to determine MW of the individual components of the receptorligand complex. The results of these determinations are as follows:
MW of the Flt1D2Flk1D3.FcΔC1(a)/VEGF165 complex at the peak
position is 157 300 (Figure 33), the MW of VEGF165 at the peak
position is 44 390 (Figure 34) and the MW of R1R2 at the peak is 113
300 (Figure 35).

Figure 36. Peptide mapping and glycosylation analysis. The disulfide structures and glycosylation sites in Flt1D2.Flk1D3.FcΔC1(a) were

25

5

determined by a peptide mapping method. There are a total of ten cysteines in Flt1D2.Flk1D3.FcΔC1(a); six of them belong to the Fc region. Cys27 is disulfide bonded to Cys76. Cys121 is disulfide bonded to Cys 182. The first two cysteines in the Fc region (Cys211 and Cys214) form an intermolecular disulfide bond with the same two cysteines in another Fc chain. However, it can not be determined whether disulfide bonding is occurring between same cysteines (Cys211 to Cys211, for example) or between Cys211 and Cys214. Cys216 is disulfide bonded to Cys306. Cys 352 is disulfide bonded to Cys410.

There are five possible N-linked glycosylation sites in Flt1D2.Flk1D3.FcΔC1(a) and are found to be glycosylated to varying degrees. Complete glycosylation is observed at Asn33, Asn193, and Asn282. Partial glycosylation is observed on Asn65 and Asn120. Sites of glycosylation are highlighted by underline in the Figure.

Figure 37. Pharmacokinetics of Flt1(1-3)-Fc (A40), Flt1D2.Flk1D3.FcΔC1(a) and VEGFR1R2-FcΔC1(a). Balb/c mice were injected subcutaneously with 4mg/kg of Flt1(1-3)-Fc (A40), CHO transiently expressed Flt1D2.Flk1D3.FcΔC1(a), CHO stably expressed Flt1D2.Flk1D3.FcΔC1(a), and CHO transiently expressed VEGFR1R2-FcΔC1(a). The mice were tail bled at 1, 2, 4, 6, 24 hrs, 2 days, 3 days and 6 days after injection. The sera were assayed in an ELISA designed to detect Flt1(1-3)-Fc (A40), Flt1D2.Flk1D3.FcΔC1(a) or VEGFR1R2-

FcΔC1(a). The Tmax for Flt1(1-3)-Fc (A40) was at 6 hrs while the Tmax for the transient and stable Flt1D2.Flk1D3.FcΔC1(a) and the transient VEGFR1R2-FcΔC1(a) was 24hrs. The Cmax for Flt1(1-3)-Fc (A40) was $8\mu g/ml$, For both transients (Flt1D2.Flk1D3.FcΔC1(a) and VEGFR1R2-FcΔC1(a)) the Cmax was $18\mu g/ml$ and the Cmax for the stable VEGFR1R2-FcΔC1(a) was $30\mu g/ml$.

Figure 38. Pharmacokinetics of Flt1(1-3)-Fc (A40), Flt1D2.Flk1D3.FcΔC1(a) and Flt1D2.VEGFR3D3.FcΔC1(a). Balb/c mice were injected subcutaneously with 4mg/kg of Flt1(1-3)-Fc (A40), CHO transiently expressed Flt1D2.Flk1D3.FcΔC1(a) and CHO transiently expressed Flt1D2.VEGFR3D3.FcΔC1(a). The mice were tail bled at 1, 2, 5, 6, 7, 8, 12, 15 and 20 days after injection. The sera were assayed in an ELISA designed to detect Flt1(1-3)-Fc, Flt1D2.Flk1D3.FcΔC1(a) and Flt1D2.VEGFR3D3.FcΔC1(a). Flt1(1-3)-Fc (A40) could no longer be detected in the serum after day 5 whereas Flt1D2.Flk1D3.FcΔC1(a) and Flt1D2.VEGFR3D3.FcΔC1(a) were detectable for 15 days or more.

Figure 39. The Ability of Flt1D2.Flk1D3.FcΔC1(a) to Inhibit HT-1080
20 Fibrosarcoma Tumor Growth In Vivo. Every other day or 2 times per
week treatment of SCID mice with Flt1D2.Flk1D3.FcΔC1(a) at 25mg/Kg
significantly decreases the growth of subcutaneous HT-1080
fibrosarcoma tumors.

Figure 40. The Ability of Flt1D2.Flk1D3.Fc\(\Delta\)C1(a) to Inhibit C6 Glioma Tumor Growth In Vivo. Every other day or 2 times a week treatment of SCID mice with Flt1D2.Flk1D3.Fc\(\Delta\)C1(a) significantly decreases the growth of subcutaneous C6 glioma tumors at doses as low as 2.5mg/Kg.

5

Figure 41. VEGF-Induced Uterine Hyperpermeability. PMSG injected subcutaneously (5 IU) to induce ovulation in prepubertal female rats results in a surge of estradiol after 2 days which in turn causes an induction of VEGF in the uterus. This induction results in hyperpermeability of the uterus and an increase in uterine wet. Subcutaneous injection of Flt1(1-3)-Fc (A40), Flt1D2.Flk1D3.Fc△C1(a) and Flt1D2.VEGFR3D3.Fc∆C1(a) at 25mg/kg at 1hr after PMSG injection results in about a 50% inhibition of the increase in uterine wet weight.

15 15

Figure 42A-42B. Assessment of Corpus Luteum Angiogenesis Using Progesterone as a Readout. PMSG was injected subcutaneously (5 IU) to induce ovulation in prepubertal female rats, resulting in a fully functioning corpus luteum containing a dense network of blood vessels that secretes progesterone into the blood stream to prepare the uterus for implantation. The induction of angiogenesis in the corpus luteum requires VEGF. Resting levels of progesterone are about 5ng/ml and can be induced to 25-40ng/ml after PMSG. Subcutaneous injection of Flt1(1-3)-Fc (A40) or Flt1D2.Flk1D3.Fc\(Delta C1(a)\) at 25mg/kg or 5mg/kg at 1hr. after PMSG injection resulted in a complete inhibition of the progesterone induction on day 4.

25

20

Figure 43: Gross phenotype of K14VEGF transgenic mice. Six months after birth, the mice develop significant skin lesions on the ears and scalp. The skin becomes red, edematous, and profoundly scaling (parakeratosis and hyperkeratosis) to the point of generalized desquamation.

Figure 44A-Figure 44C: Histology of ear skin from K14VEGF transgenic mice (hematoxylin and eosin stained sections).

Figure 44A: Control, nontransgenic wildtype mouse. Figure 44B: K14VEGF transgenic mouse at three months of age. Figure 44C: K14VEGF transgenic mouse at six months of age. Note thickening of epidermis with increased hyperkeratosis and parakeratosis (40X).

Figure 45: Rete ridge formation in relatively mature psoriatic-like lesions in K14VEGF transgenic mice (Masson's Trichrome staining). K14VEGF transgenic mouse at 6 months of age has developed dramatic rete ridge structures, some of which are fused at the base (4x).

Figure 46A-46B: Formation of microabscesses in relatively mature psoriatic-like lesions in K14VEGF transgenic mice. (Hematoxylin and eosin staining of skin sections from K14VEGF transgenic mice at 6 months of age.) Figure 46A: Monro microabscess. Figure 46B: Kogoj microabscess.

20

5



Figure 47A-47P: Effect of VEGFR1R2-FcΔC1(a) in an animal model of psoriasis. A K14VEGF transgenic mouse with severe skin lesions was injected with VEGFR1R2-FcΔC1(a) (25 mg/kg) on day 0 (Fig. 47A-47D), day 3 (Fig. 47E-47H), day 7 (Fig. 47I - 47L), and day10 (Fig. 47M-47P), and photographed after each injection.

<u>DETAILED DESCRIPTION OF THE INVENTION</u>

It has been a long standing problem in the art to produce a receptor based VEGF antagonist that has a pharmacokinetic profile that is appropriate for consideration of the antagonist as a therapeutic candidate. Applicants describe herein, for the first time, a chimeric polypeptide molecule, capable of antagonizing VEGF activity, that exhibits improved pharmacokinetic properties as compared to other known receptor-based VEGF antagonists. The chimeric polypeptide molecules described herein thus provide for the first time appropriate molecules for use in therapies in which antagonism of VEGF is a desired result.

The present invention provides for novel chimeric polypeptide molecules formed by fusing a modified extracellular ligand binding domain of the Elt1 receptor to the Fc region of IgG.

The extracellular ligand binding domain is defined as the portion of a receptor that, in its native conformation in the cell membrane, is oriented extracellularly where it can contact with its cognate ligand.

5

The extracellular ligand binding domain does not include the hydrophobic amino acids associated with the receptor's transmembrane domain or any amino acids associated with the receptor's intracellular Generally, the intracellular or cytoplasmic domain of a domain. receptor is usually composed of positively charged or polar amino acids (i.e. lysine, arginine, histidine, glutamic acid, aspartic acid). preceding 15-30, predominantly hydrophobic or apolar amino acids (i.e. leucine, valine, isoleucine, and phenylalanine) comprise the transmembrane domain. The extracellular domain comprises the amino acids that precede the hydrophobic transmembrane stretch of amino acids. Usually the transmembrane domain is flanked by positively charged or polar amino acids such as lysine or arginine. von Heijne has published detailed rules that are commonly referred to by skilled artisans when determining which amino acids of a given receptor belong to the extracellular, transmembrane, or intracellular domains (See von Heijne, 1995, BioEssays 17:25-30). Alternatively, websites on the Internet, such as http://ulrec3.unil.ch/software/TMPRED_form.html. have become available to provide protein chemists with information about making

predictions about protein domains.

2.0

25

5

The present invention provides for the construction of nucleic acid molecules encoding chimeric polypeptide molecules that are inserted into a vector that is able to express the chimeric polypeptide molecules when introduced into an appropriate host cell. Appropriate host cells include, but are not limited to, bacterial cells, yeast cells, insect cells, and mammalian cells. Any of the methods known to one skilled in the art for the insertion of DNA fragments into a vector may be used to construct expression vectors encoding the chimeric polypeptide molecules under control of transcriptional/translational control signals. These methods may include in vitro recombinant DNA and synthetic techniques and in vivo recombinations (genetic recombination) (See Sambrook, et al., Molecular Cloning, A Laboratory Manual, Cold Spring Harbor Laboratory; Current Protocols in Molecular Biology, Eds. Ausubel, et al., Greene Publ. Assoc., Wiley-Interscience, NY).

Expression of nucleic acid molecules encoding the chimeric polypeptide molecules may be regulated by a second nucleic acid sequence so that the chimeric polypeptide molecule is expressed in a host transformed with the recombinant DNA molecule. For example, expression of the chimeric polypeptide molecules described herein may be controlled by any promoter/enhancer element known in the art. Promoters which may be used to control expression of the chimeric polypeptide molecules include, but are not limited to, the long terminal repeat as described in Squinto et al., (1991, Cell 65:1-20); the SV40 early promoter region

25

5

(Bernoist and Chambon, 1981, Nature 290:304-310), the CMV promoter, the M-MuLV 5' terminal repeat the promoter contained in the 3' long terminal repeat of Rous sarcoma virus (Yamamoto, et al., 1980, Cell 22:787-797), the herpes thymidine kinase promoter (Wagner et al., 1981, Proc. Natl. Acad. Sci. U.S.A. 78:144-1445), the regulatory sequences of the metallothionine gene (Brinster et al., 1982, Nature 296:39-42); prokaryotic expression vectors such as the β -lactamase promoter (Villa-Kamaroff, et al., 1978, Proc. Natl. Acad. Sci. U.S.A. 75:3727-3731), or the tac promoter (DeBoer, et al., 1983, Proc. Natl. Acad. Sci. U.S.A. 80:21-25, see also "Useful proteins from recombinant bacteria" in Scientific American, 1980, 242:74-94); promoter elements from yeast or other fungi such as the Gal 4 promoter, the ADH (alcohol dehydrogenase) promoter, PGK (phosphoglycerol kinase) promoter, alkaline phosphatase promoter, and the following animal transcriptional control regions, which exhibit tissue specificity and have been utilized in transgenic animals: elastase I gene control region which is active in pancreatic acinar cells (Swift et al., 1984, Cell 38:639-646; Ornitz et al., 1986, Cold Spring Harbor Symp. Quant. Biol. 50:399-409; MacDonald, 1987, Hepatology 7:425-515); insulin gene control region which is active in pancreatic beta cells (Hanahan, 1985, Nature 315:115-122), immunoglobulin gene control region which is active in lymphoid cells (Grosschedl et al., 1984, Cell 38:647-658; Adames et al., 1985, Nature 318:533-538; Alexander et al., 1987, Mol. Cell. Biol. 7:1436-1444), mouse mammary tumor virus control region which is active in testicular, breast, lymphoid and mast cells (Leder et

25

5

al., 1986, Cell 45:485-495), albumin gene control region which is active in liver (Pinkert et al., 1987, Genes and Devel. 1:268-276), alpha-fetoprotein gene control region which is active in liver (Krumlauf et al., 1985, Mol. Cell. Biol. 5:1639-1648; Hammer et al., 1987, Science 235:53-58); alpha 1-antitrypsin gene control region which is active in the liver (Kelsey et al, 1987, Genes and Devel. 1:161-171), beta-globin gene control region which is active in myeloid cells (Mogram et al., 1985, Nature 315:338-340; Kollias et al., 1986, Cell 46:89-94); myelin basic protein gene control region which is active in oligodendrocyte cells in the brain (Readhead et al., 1987, Cell 48:703-712); myosin light chain-2 gene control region which is active in skeletal muscle (Shani, 1985, Nature 314:283-286), and gonadotropic releasing hormone gene control region which is active in the hypothalamus (Mason et al., 1986, Science 234:1372-1378).

Thus, according to the invention, expression vectors capable of being replicated in a bacterial or eukaryotic host comprising chimeric polypeptide molecule-encoding nucleic acid as described herein, are used to transfect the host and thereby direct expression of such nucleic acids to produce the chimeric polypeptide molecules, which may then be recovered in a biologically active form. As used herein, a biologically active form includes a form capable of binding to VEGF.

Expression vectors containing the chimeric nucleic acid molecules described herein can be identified by three general approaches: (a)

5

DNA-DNA hybridization, (b) presence or absence of "marker" gene functions, and (c) expression of inserted sequences. In the first approach, the presence of a foreign gene inserted in an expression vector can be detected by DNA-DNA hybridization using probes comprising sequences that are homologous to the inserted chimeric polypeptide molecule sequences. In the second approach, the recombinant vector/host system can be identified and selected based upon the presence or absence of certain "marker" gene functions (e.g., thymidine kinase activity, resistance to antibiotics, transformation phenotype, occlusion body formation in baculovirus, etc.) caused by the insertion of foreign genes in the vector. For example, if the chimeric polypeptide molecule DNA sequence is inserted within the marker gene sequence of the vector, recombinants containing the insert can be identified by the absence of the marker gene function. In the third approach, recombinant expression vectors can be identified by assaying the foreign gene product expressed by the recombinant. Such assays can be based, for example, on the physical or functional properties of the chimeric polypeptide molecules.

Cells of the present invention may transiently or, preferably, constitutively and permanently express the chimeric polypeptide molecules.

The chimeric polypeptide molecules may be purified by any technique which allows for the subsequent formation of a stable, biologically

active chimeric polypeptide molecule. For example, and not by way of limitation, the factors may be recovered from cells either as soluble proteins or as inclusion bodies, from which they may be extracted quantitatively by 8M guanidinium hydrochloride and dialysis (see, for example, Builder, et al., US Patent No. 5,663,304). In order to further purify the factors, conventional ion exchange chromatography, hydrophobic interaction chromatography, reverse phase chromatography or gel filtration may be used.

In one embodiment of the invention, the nucleotide sequence encoding the first component is upstream of the nucleotide sequence encoding the second component. In another embodiment of the invention, the nucleotide sequence encoding the first component is downstream of the nucleotide sequence encoding the second component. Further embodiments of the invention may be prepared in which the order of the first, second and third fusion polypeptide components are rearranged. For example, if the nucleotide sequence encoding the first component is designated 1, the nucleotide sequence encoding the second component is designated 2, and the nucleotide sequence of the third component is designated 3, then the order of the components in the isolated nucleic acid of the invention as read from 5' to 3' may be any of the following six combinations: 1,2,3; 1,3,2; 2,1,3; 2,3,1; 3,1,2; or 3,2,1.

The present invention also has diagnostic and therapeutic utilities. In particular embodiments of the invention, methods of detecting

aberrancies in the function or expression of the chimeric polypeptide molecules described herein may be used in the diagnosis of disorders. In other embodiments, manipulation of the chimeric polypeptide molecules or agonists or antagonists which bind the chimeric polypeptide molecules may be used in the treatment of diseases. In further embodiments, the chimeric polypeptide molecule is utilized as an agent to block the binding of a binding agent to its target.

By way of example, but not limitation, the method of the invention may be useful in treating clinical conditions that are characterized by vascular permeability, edema or inflammation such as brain edema associated with injury, stroke or tumor; edema associated with inflammatory disorders such as psoriasis or arthritis, including rheumatoid arthritis; asthma; generalized edema associated with burns; ascites and pleural effusion associated with tumors, inflammation or trauma; chronic airway inflammation; capillary leak syndrome; sepsis; kidney disease associated with increased leakage of protein; and eye disorders such as age related macular degeneration and diabetic retinopathy.

20

25

An amino acid sequence analysis of Flt1(1-3)-Fc revealed the presence of an unusually high number (46) of the basic amino acid residue lysine. An IEF analysis of Flt1(1-3)-Fc showed that this protein has pl greater than 9.3, confirming the prediction that the protein is very basic. It was hypothesized that the basic nature of Flt1(1-3)-Fc protein was

25

5

causing it to bind to extracellular matrix components and that this interaction might be the cause of the extremely short detectable circulating serum half-life exhibited by Flt1(1-3)-Fc when injected into mice. In order to test this hypothesis, Flt1(1-3)-Fc protein was acetylated at the lysine residues to reduce the basic charge.

Acetylated Flt1(1-3)-Fc was then tested in the assays described *infra*.

The following examples are offered by way of illustration and not by way of limitation.

EXAMPLES

Example 1: Expression of Flt1(1-3)-Fc protein in CHO K1 cells.

Using standard molecular biology techniques (see e.g., Molecular Cloning, A Laboratory Manual (Sambrook, et al., Cold Spring Harbor Laboratory), Current Protocols in Molecular Biology (Eds. Ausubel, et al., Greene Publ. Assoc., Wiley-Interscience, NY), the gene encoding Flt1(1-3)-Fc was inserted into the expression vector pEE14.1 (Lonza Biologics, plc) at a multiple cloning site downstream of the CMV promoter. CHO K1 cells were transfected with the pEE14.1/Flt1(1-3)-Fc DNA construct using lipofectamine (Gaithersburg, MD). The transfected CHO K1 cells were grown in glutamine-free DMEM (JRH, Kansas City, MO) containing 25µM methionine sulfoximine (MSX) from Sigma Inc., St. Louis, MO, and high recombinant protein expressors were obtained by

5

screening the CHO K1 cell supernatants from over 100 hand-picked colony isolates using a standard immunoassay which captures and detects human Fc. The selected hand-picked clone was amplified in the presence of 100 μ M MSX followed by a second round of screening of the amplified clones. The highest producing clone had a specific productivity of recombinant Flt1(1-3)-Fc protein of 55 pg/cell/day.

The selected clone was expanded in 225cm² T-flasks (Corning, Acton, MA) and then into 8.5L roller bottles (Corning, Acton, MA) using the cell culture media described supra. Cells were removed from the roller bottles by standard trypsinization and put into 3.5L of suspension medium. The suspension medium is comprised of glutamine-free ISCHO medium (Irvine Scientific, Santa Ana, CA) containing 5% fetal bovine serum (FBS from Hyclone Labs, Logan, UT), 100µM MSX and GS supplement (JRH Scientific, Kansas City, MO) in a 5L Celligen bioreactor (New Brunswick Scientific, New Brunswick, NJ) at a density of 0.3 x 10⁶ cells/mL. After the cells reached a density of 3.6 x 10⁶/mL and were adapted to suspension they were transferred to a 60L bioreactor (ABEC, Allentown, PA) at a density of 0.5 x 10⁶ cells/mL in 20L of ISCHO medium with 5% fetal bovine serum. After two days an additional 20L of ISCHO + 5% fetal bovine serum was added to the bioreactor. The cells were allowed to grow for an additional two days reaching a final density of 3.1 x 10⁶ cells/mL, and a final Flt1(1-3)-Fc

concentration at harvest was 95 mg/L. At harvest the cells were removed by tangential flow filtration using $0.45\mu m$ Prostak Filters (Millipore, Inc., Bedford, MA).

5 Example 2: Purification of Flt1(1-3)-Fc protein obtained from CHO K1 cells

Flt1(1-3)-Fc protein was initially purified by affinity chromatography. A Protein A column was used to bind, with high specificity, the Fc portion of the molecule. This affinity-purified protein was then concentrated and passed over a SEC column. The protein was then eluted into the formulation buffer. The following describes these procedures in detail.

Materials and Methods

All chemicals were obtained from J.T. Baker, Phillipsburg, NJ with the exception of PBS, which was obtained as a 10X concentrate from Life Technologies, Gaithersburg, MD. Protein A Fast Flow and Superdex 200 preparation grade resins were obtained from Pharmacia, Piscataway, NJ. Equipment and membranes for protein concentration were obtained from Millipore, Bedford, MA.

Approximately 40L of 0.45µm-filtered CHO conditioned media containing Flt1(1-3)-Fc protein was applied to a 290mL Protein A Fast

5

Flow column (10cm diameter) that had been equilibrated with PBS. The column was washed with PBS containing 350mM NaCl and 0.02% CHAPS and the bound protein was eluted with 20mM Citric Acid containing 10mM Na₂HPO₄. The single peak in the elution was collected and its pH was raised to neutrality with 1M NaOH. The eluate fractions was concentrated to approximately 9 mg/mL using 10K regenerated cellulose membranes by both tangential flow filtration and by stirred cell concentration. To remove aggregates and other contaminants, the concentrated protein was applied to a column packed with Superdex 200 preparation grade resin (10cm x 55cm) and run in PBS containing 5 % glycerol. The main peak fractions were pooled, sterile filtered, aliquoted and stored at -80°C.

Example 3: Acetylation of Fit1(1-3)-Fc protein.

Two milligrams of Flt1(1-3)-Fc protein were acetylated as described in the instruction manual provided with the sulfo-NHS-acetate modification kit (Pierce Chemical Co., Rockford, IL, Cat.#26777).

20 Example 4: Characterization of acetylated Flt1(1-3)-Fc protein.

(a.) IEF analysis: Flt1(1-3)-Fc and acetylated Flt1(1-3)-Fc were analyzed by standard IEF analysis. As shown in Figure 1, Flt1(1-3)-Fc protein is not able to migrate into the gel and therefore must have a pl

25

5

greater than 9.3, the highest pl in the standard. However, acetylated Flt1(1-3)-Fc is able to migrate into the gel and equilibrate at a pl of approximately 5.2. This result demonstrates that acetylation reduces the net positive charge of the protein and therefore its pl considerably.

(b.) Binding to extracellular matrix components

To test for binding to extracellular matrix components, Flt1(1-3)-Fc and acetylated Flt1(1-3)-Fc where tested in an assay designed to mimic the interaction with extracellular matrix components. In this assay, 96-well tissue culture plates are coated with Matrigel (Biocoat MATRIGEL® matrix thin layer 96 well plate, Catalog #40607, Becton Dickinson Labware, Bedford, MA). The plates are incubated with varying concentrations of either Flt1(1-3)-Fc, acetylated Flt1(1-3)-Fc, or rTie2-Fc (an irrelevant control) protein are added to the wells. The plates are incubated for 1-2 hours at either room temperature or 37°C degrees and then detection of bound proteins is accomplished by adding a secondary alkaline phosphatase-conjugated anti-human Fc antibody to the wells. Finally, alkaline phosphatase substrate is added to the wells and optical density is measured. Figure 2 shows the results of this assay. Like the irrelevant control protein rTie2-Fc, acetylated Flt1(1-3)-Fc does not exhibit any binding to the Matrigel coated plate, whereas the non-acetylated Flt1(1-3)-Fc protein exhibits significant binding. This result indicates that acetylation of basic amino acid residues is an effective way to interfere with the charge interactions that exist

5

between positively charged proteins and the negatively charged extracellular matrix components they are exposed to in vivo.

Example 5: Pegylation of Flt1(1-3)-Fc protein.

Although pegylation (polyethylene glycol - PEG) of proteins has been shown to increase their *in vivo* potency by enhancing stability and bioavailability while minimizing immunogenicity (see references cited *supra*), it is counter-intuitive that pegylating molecules that are too large to be filtered by the kidney glomeruli would improve their pharmacokinetic properties. Without being bound by theory, Applicants postulated that pegylation of the Flt1(1-3)-Fc molecules could improve the pharmacokinetic properties, possibly not by altering the positive charge or by decreasing the pl of Flt1(1-3)-Fc, but rather by physically shielding the positive charges from interacting with the extracellular matrix. Applicants decided to attempt to improve the pharmacokinetic properties of Flt1(1-3)-Fc molecules by attaching strands of 20K PEGs as described *infra*.

20 Materials and Methods

Purified Flt1(1-3)-Fc derived from CHO cells (see *supra*) was used in the following pegylation experiments. Functionalized PEGs were obtained from Shearwater Polymers, Huntsville, AL; Bicine from Sigma, St Louis, MO; Superose 6 column from Pharmacia, Piscataway, NJ; PBS

5

as a 10X concentrate from Life Technologies, Gaithersburg, MD; Glycerol from J.T. Baker, Phillipsburg, NJ; and Bis-Tris precast gels from Novex, CA.

20K PEG strands functionalized with amine-specific terminal moieties were used in small-scale reaction studies that were set-up to evaluate different reaction conditions in which the PEG:protein stoichiometry was varied. Based on these reactions and the analyses of samples on standard SDS-PAGE, Flt1(1-3)-Fc at a concentration of 1.5 mg/mL was reacted at pH 8.1 with 20K SPA-PEG (PEG succinimidyl propionate) molecules at a PEG-to-Flt1(1-3)-Fc monomer molar ratio of 1:6. The reaction was allowed to proceed at 8°C overnight. For initial purification, the reaction products were applied to a 10mm x 30cm Superose 6 column equilibrated with PBS containing 5% Glycerol. column appeared to separate pegylated Flt1(1-3)-Fc molecules based on the extent of pegylation. Fractions corresponding to what appeared to be primarily mono-pegylated and di-pegylated dimeric Flt1(1-3)-Fc, as judged by banding patterns on reducing and non-reducing SDS-PAGE gels were pooled. The protein concentration was determined by measuring absorbance at 280 nm. The pegylated Flt1(1-3)-Fc protein was sterile filtered, aliquoted and stored at -40°C.

25

5

Exampl 6: Binding of unmodified, acetylated, and pegylated Flt1(1-3)-Fc in a Biacore-based assay.

Unmodified, acetylated, and pegylated Flt1(1-3)-Fc proteins were tested in a Biacore-based assay to evaluate their ability to bind to the Flt1 ligand, VEGF. In this assay, unmodified Flt1(1-3)-Fc protein was immobilized on the surface of a Biacore chip (see Biacore Instruction Manual, Pharmacia, Inc., Piscataway, NJ, for standard procedures) and a sample containing 0.2 μ g/ml VEGF and either unmodified Flt1(1-3)-Fc, acetylated Flt1(1-3)-Fc or pegylated Flt1(1-3)-Fc (each at 25 μ g/ml) was passed over the Flt1(1-3)-Fc-coated chip. To minimize the effects of non-specific binding, the bound samples were washed with a 0.5M NaCl wash. In one sample, unmodified Flt1(1-3)-Fc was mixed with heparin. Heparin is a negatively charged molecule and the Flt1(1-3)-Fc protein is a positively charged molecule, so when the two molecules are mixed together, they should interact through their respective This essentially neutralizes Flt1(1-3)-Fc's inherent positive charges. charge making the molecule behave as if it has been chemically or genetically modified so as to reduce its charge and its tendency to bind via charge interactions. As shown in Figure 3, acetylated (columns 13-16), pegylated (columns 17-20), and heparin-treated Flt1(1-3)-Fc (columns 21-24) are each able to completely compete with the Biacore chip-bound Flt1(1-3)-Fc for VEGF binding as compared to control (columns 1-4) and irrelevant protein (columns 5-8). Unmodified Flt1(1-3)-Fc (columns 5-6) appeared to only partially compete with

Biacore chip-bound Flt1(1-3)-Fc for VEGF binding. However, washing the bound samples with 0.5M NaCl (columns 7-8) resulted in a binding profile similar to the modified forms of Flt1(1-3)-Fc, indicating that the unmodified protein was exhibiting non-specific binding to the chip that could be eliminated by the salt wash.

Example 7: Binding of unmodified, acetylated, and pegylated Flt1(1-3)-Fc in an ELISA-based assay.

Unmodified, acetylated, and pegylated Flt1(1-3)-Fc proteins were tested in a standard ELISA-based assay to evaluate their ability to bind the Flt1 receptor ligand VEGF. As shown in Figure 4, both pegylated and acetylated Flt1(1-3)-Fc proteins are capable of binding to VEGF, demonstrating that modifying the protein either by pegylation or acetylation does not destroy its ability to bind its ligand.

Example 8: Pharmacokinetic analysis of unmodified Flt1(1-3)-Fc, acetylated Flt1(1-3)-Fc, and pegylated Flt1(1-3)-Fc.

In vivo experiments were designed to assess the pharmacokinetic profiles of unmodified Flt1(1-3)-Fc, acetylated Flt1(1-3)-Fc, and pegylated Flt1(1-3)-Fc protein. Balb/c mice (23-28g; 3 mice/group) were injected subcutaneously with 4mg/kg of unmodified, acetylated, or pegylated Flt1(1-3)-Fc. The mice were tail bled at 1, 2, 4, 6, 24 hours, 2 days, and 3 days after injection of protein. The sera were assayed in a standard ELISA-based assay designed to detect Flt1(1-3)-

Fc protein. Briefly, the assay involves coating an ELISA plate with VEGF, binding the unmodified, acetylated, or pegylated Flt1(1-3)-Fc-containing sera, and reporting with an anti-Fc antibody linked to alkaline phosphatase. As shown in Figure 5, the Tmax for all of the Flt1(1-3)-Fc proteins was between the 6 hour and 24 hour time points. The Cmax for the different proteins was as follows: Unmodified: 0.06 μ /ml - 0.15 μ g/ml; acetylated: 1.5 μ g/ml - 4.0 μ g/ml; and pegylated: approximately 5 μ g/ml.

Example 9: Step-acetylation of Flt1(1-3)-Fc

To determine what minimal amount of acetylation is necessary to eliminate binding to extracellular matrix components, an experiment was designed that acetylated the Flt1(1-3)-Fc protein in a step-wise fashion by using increasing amounts of molar excess of acetylation reagent in the acetylation reaction mixture. The range of molar excess was as follows: 0, 10, 20, 30, 40, 50, 60, 70, 80, 90, and 100 moles of acetylation reagent per 1 mole of Flt1(1-3)-Fc monomer. The reactions were performed as detailed in the instruction manual provided with the sulfo-NHS-Acetate modification kit (Pierce Chemical Co., Rockford, IL, Cat.# 26777).

25

5

Example 10: Characterization of step-acetylated Flt1(1-3)-Fc.

(a.) IEF analysis Unmodified Flt1(1-3)-Fc and step-acetylated Flt1(1-3)-Fc proteins were analyzed by standard IEF analysis. As shown in Figure 6A-6B, unmodified Flt1(1-3)-Fc protein was not able to migrate into the gel due to its extremely high pl (greater than 9.3). However, most of the step-acetylated Flt1(1-3)-Fc samples (30-100 fold molar excess samples) were able to migrate into the gel and equilibrate at pls ranging between 4.55 - 8.43, depending on the degree of acetylation of the protein. This result demonstrates that acetylation can change the positive charge of the protein in a dosedependent manner and that reduction of the pl can be controlled by controlling the degree of acetylation.

(b.) Binding of step-acetylated Flt1(1-3)-Fc to extracellular matrix components

To test for binding to extracellular matrix components, Flt1(1-3)-Fc and step-acetylated Flt1(1-3)-Fc where tested in the above-described assay designed to mimic the interaction with extracellular matrix components. Varying concentrations of either unmodified Flt1(1-3)-Fc, step-acetylated Flt1(1-3)-Fc (10, 20, and 30 fold molar excess samples), or rTie2-Fc (an irrelevant control) protein were added to the wells. The plates were incubated for 1-2 hours at room temperature or 37°C and then detection of bound proteins was accomplished by adding a

5

secondary alkaline phosphatase-conjugated anti-human Fc antibody to the wells. Alkaline phosphatase substrate was subsequently added to the wells and optical density measured. Figure 7 shows the results of this assay. Like the irrelevant control protein rTie2-Fc, stepacetylated Flt1(1-3)-Fc (20 and 30 fold molar excess samples) did not exhibit any significant binding to the Matrigel coated plate, whereas the non-acetylated Flt1(1-3)-Fc protein exhibited significant binding. The binding is saturable, indicating that the Flt1(1-3)-Fc protein may be binding to specific sites, rather than a more general chargemediated interaction that might not be saturable. The 10 fold molar excess sample showed reduced binding, but the degree of acetylation was not enough to completely block binding to extracellular matrix components. The 20 fold molar excess and higher samples displayed no detectable binding, despite the fact that by IEF analysis (Figure 6A and 6B) the lower molar excess samples still had a large net positive This result demonstrates that it is not necessary to completely acetylate all available basic amino acids in order to eliminate binding to extracellular matrix components.

20 (c.) Binding of step-acetylated Flt1(1-3)-Fc in a Biacore-based assay.

Unmodified and step-acetylated Flt1(1-3)-Fc proteins where tested in a Biacore-based assay to evaluate their ability to bind to the Flt1 ligand, VEGF. In this assay, unmodified Flt1(1-3)-Fc protein (0.5, 1.0,

or 5.0 μ g/ml) was immobilized on the surface of a Biacore chip (see Biacore Instruction Manual, Pharmacia, Inc., Piscataway, NJ, for standard procedures) and a solution containing 0.2 μ g/ml VEGF and either unmodified Flt1(1-3)-Fc (at either 0.5, 1.0, or 5.0 μ g/ml) or 10 different step-acetylated Flt1(1-3)-Fc samples (at 0.5, 1.0, or 5.0 μ g/ml each) were passed over the Flt1(1-3)-Fc-coated chip. As shown in Figure 8, at a sub-stoichiometric ratio (0.5 μ g/ml of either unmodified Flt1(1-3) or step-acetylated Flt1(1-3)-Fc vs. 0.2 μ g/ml · VEGF), there is not enough Flt1(1-3)-Fc (either unmodified or stepacetylated) in the solution to completely bind the VEGF. At 1.0 μ g/ml, which approximates a 1:1 stoichiometric ratio, both unmodified and step-acetylated Flt1(1-3)-Fc are better able to compete for VEGF binding, but there is still insufficient Flt1(1-3)-Fc protein (either unmodified or step-acetylated) to completely bind the available VEGF. However, at 5.0 μ g/ml, which is several times greater than a 1:1 stoichiometric ratio, both the Flt1(1-3)-Fc and the step-acetylated Flt1(1-3)-Fc proteins are able to bind the VEGF, regardless of the degree of acetylation. This clearly demonstrates that acetylation does not alter Flt1(1-3)-Fc's ability to bind VEGF.

20

25

(d.) Pharmacokinetic analysis of step-acetylated Flt1(1-3)-Fc

In vivo experiments were designed to assess the pharmacokinetic profiles of unmodified Flt1(1-3)-Fc and step-acetylated Flt1(1-3)-Fc protein. Balb/c mice (23-28g) were injected subcutaneously with

25

5

4mg/kg of unmodified or 10, 20, 40, 60 and 100 fold molar excess samples of step-acetylated Flt1(1-3)-Fc (3 mice for unmodified, 10, 20 and 40 fold molar excess samples and 2 mice for 60 and 100 fold molar excess samples). The mice were tail bled at 1, 2, 4, 6, 24 hours, 2 days and 3 days after injection. The sera were assayed in an ELISA-based assay designed to detect Flt1(1-3)-Fc (described supra). Figure 9 details the results of this study. The Tmax for all of the Flt1(1-3)-Fc proteins tested was at the 6 hour time point but the Cmax was as follows: Unmodified Flt1(1-3)-Fc: $0.06\mu g/ml$; 10 fold molar excess sample: $-0.7\mu g/ml$, 20 fold molar excess sample $-2\mu g/ml$, 40 fold molar excess sample $-4\mu g/ml$, 60 fold molar excess sample $-2\mu g/ml$, 100 fold molar excess sample $-1\mu g/ml$. This results demonstrates that acetylation or pegylation of Flt1(1-3)-Fc significantly improves its pharmacokinetic profile.

Example 11: Construction of Flt1(1-3)-Fc basic region deletion mutant designated Mut1: Flt1(1-3 $_{\Delta B}$)-Fc.

Based on the observation that acetylated Flt1(1-3)-Fc, which has a pl below 6, has much better pharmacokinetics than the highly positive unmodified Flt1(1-3)-Fc (pl > 9.3), it was asked whether the difference in pharmacokinetics could be attributed to the net charge of the protein, which made it stick to negatively charged extracellular matrix components, or whether there were perhaps specific locations on the surface of the Flt1(1-3)-Fc protein that constituted specific binding

25

5

sites for extracellular matrix components. For example, many proteins are known to have heparin binding sites, often consisting of a cluster of basic residues. Sometimes these residues are found in a cluster on the primary sequence of the protein; some of the literature has identified "consensus sequences" for such heparin binding sites (see for example Hileman, et al., 1998, Bioessays 20(2):156-67). In other cases, the known crystal structure of a protein reveals a cluster of positively charged residues on the surface of a protein, but the residues come from different regions of the primary sequence and are only brought together when the protein folds into its tertiary structure. difficult to deduce whether an isolated amino acid residue forms part of a cluster of basic residues on the surface of the protein. However, if there is a cluster of positively charged amino acid residues in the primary sequence, it is not unreasonable to surmise that the residues are spatially close to one another and might therefore be part of an extracellular matrix component binding site. Flt1 receptor has been studied extensively and various domains have been described (see for example Tanaka et al., 1997, Jpn. J. Cancer Res 88:867-876). Referring to the nucleic acid and amino acid sequence set forth in Figure 10A-10D of this application, one can identify the signal sequence for secretion which is located at the beginning of the sequence and extends to the glycine coded for by nucleotides 76-78. The mature protein begins with Ser-Lys-Leu-Lys, starting at nucleotide 79 of the nucleic acid sequence. Flt1 Ig domain 1 extends from nucleotide 79 to 393, ending with the amino acids Ser-Asp-Thr. Flt1 lg domain 2 extends from

25

5

nucleotide 394 to 687 (encoding Gly-Arg-Pro to Asn-Thr-IIe), and Flt1 Ig domain 3 extends from nucleotides 688 to 996 (encoding IIe-Asp-Val to Asp-Lys-Ala). There is a bridging amino acid sequence, Gly-Pro-Gly, encoded by nucleotides 997-1005, followed by the nucleotide sequence encoding human Fc (nucleotides 1006-1701 or amino acids Glu-Pro-Lys to Pro-Gly-Lys-stop).

A more detailed analysis of the Flt1 amino acid sequence reveals that there is a cluster, namely, amino acid residues 272-281 (KNKRASVRR) of Figure 10A-10D, in which 6 out of 10 amino acid residues are basic. This sequence is located in Flt1 Ig domain 3 of the receptor (see Figure 11), which is not itself essential for binding of VEGF ligand, but which confers a higher affinity binding to ligand. An alignment of the sequence of Ig domain 3 with that of Ig domain 2 reveals that in this region, there is very poor alignment between the two lg domains, and that there are about 10 additional amino acids in Ig domain 3. An analysis of the hydrophilicity profiles (MacVector computer software) of these two domains clearly indicates the presence of a hydrophilic region in the protein (Figure 12A-12B). These observations raised the possibility that the actual three dimensional conformation of Flt1 Ig domain 3 allowed for some type of protrusion that is not in Flt1 lg domain 2. To test this hypothesis, the 10 additional amino acids were deleted and the resulting protein was tested to see whether the deletion would affect the pharmacokinetics favorably without seriously compromising the affinity of the receptor for VEGF. This DNA

construct, which was constructed using standard molecular biology techniques (see e.g., Molecular Cloning, A Laboratory Manual (Sambrook, et al., Cold Spring Harbor Laboratory), Current Protocols in Molecular Biology (Eds. Ausubel, et al., Greene Publ. Assoc., Wiley-Interscience, NY) in the mammalian expression vector pMT21 (Genetics Institute, Inc., Cambridge, MA), is referred to as Mut1: Flt1(1-3 $_{\Delta B}$)-Fc. The Mut1: Flt1(1-3 $_{\Delta B}$)-Fc construct was derived from Flt1(1-3)-Fc by deletion of nucleotides 814-843 (set forth in Figure 10A-10D), which deletes the highly basic 10-amino acid residue sequence Lys-Asn-Lys-Arg-Ala-Ser-Val-Arg-Arg-Arg from Flt1 Ig domain 3.

The final DNA construct was sequence-verified using an ABI 373A DNA sequencer and Taq Dideoxy Terminator Cycle Sequencing Kit (Applied Biosystems, Inc., Foster City, CA). The sequence of Mut1: Flt1(1-3 $_{\Delta B}$)-Fc is set forth in Figure 13A-13D.

Example 12: Construction of FIt1(1-3)-Fc basic region deletion mutant designated Mut2: FIt1(2-3 $_{\Delta B}$)-Fc.

A second deletion mutant construct, designated Mut2: $Flt1(2-3_{\Delta B})$ -Fc, was derived from the Mut1: $Flt1(1-3_{\Delta B})$ -Fc construct by deletion of Flt1 lg domain 1 encoded by nucleotides 79-393 (see Figure 10A-10D); for convenience, nucleotides 73-78 (TCA GGT) were changed to TCC GGA. This introduced a restriction site (BspE1) without altering the associated amino acid sequence, Ser-Gly. This DNA construct, which

5

was constructed using standard molecular biology techniques (see e.g., Molecular Cloning, A Laboratory Manual (Sambrook, et al., Cold Spring Harbor Laboratory), Current Protocols in Molecular Biology (Eds. Ausubel, et al., Greene Publ. Assoc., Wiley-Interscience, NY) in the mammalian expression vector pMT21 (Genetics Institute, Inc., Cambridge, MA), was also sequence-verified using an ABI 373A DNA sequencer and Taq Dideoxy Terminator Cycle Sequencing Kit (Applied Biosystems, Inc., Foster City, CA). The sequence of Mut2: Flt1(2-3 $_{\Delta B}$)-Fc is set forth in Figure 14A-14C.

Example 13: Construction of Flt1(1-3)-Fc deletion mutant designated Mut3: Flt1(2-3)-Fc.

A third deletion mutate construct, designated Mut3: Flt1(2-3)-Fc, was constructed the same way as the Mut2: Flt1(2-3 $_{\Delta B}$)-Fc construct, except that Flt1 Ig domain 3 was left intact (the basic region amino acids were not deleted). The construct was constructed using standard molecular biology techniques and the final construct was sequence-verified as described *supra*. The sequence of Mut3: Flt1(2-3)-Fc is set forth in Figure 15A-15C.

Example 14: Construction of Flt(1-3)-Fc basic region N - glycosylation mutant designated Mut4: Flt1(1-3 R->N)-Fc.

A final construct was made in which a N-glycosylation site was introduced into the middle of the basic region of Flt1 Ig domain 3. This

25

5

construct was designated Mut4: $Flt1(1-3_{R->N})$ -Fc and was made by changing nucleotides 824-825 from GA to AC, consequently changing the coded Arg residue (AGA) into an Asn residue (AAC) (see Figure 10A-10D). The resulting amino acid sequence is therefore changed from Arg-Ala-Ser to Asn-Ala-Ser, which matches the canonical signal (Asn-Xxx-Ser/Thr) for the addition of a N-glycosylation site at the Asn residue. The sequence of Mut4: $Flt1(1-3_{R->N})$ -Fc is set forth in Figure 16A-16D.

Example 15: Characterization of acetylated Flt1(1-3)-Fc, Mut1: Flt1(1-3_{AB})-Fc, and Mut4: Flt1(1-3_{R->N})-Fc mutants.

(a.) Binding to extracellular matrix components

To determine whether the three modified proteins were more or less likely to have improved pharmacokinetic properties, Matrigel coated 96-well dishes (as described supra) were incubated with varying concentrations of the mutant proteins and detected with anti-human Fc/alkaline-phosphatase conjugated antibodies. As shown in Figure 18, this experiment showed that while the unmodified Flt1(1-3)-Fc protein could bind avidly to these wells, the Mut3: Flt1(2-3)-Fc protein bound somewhat more weakly, the Mut1: Flt1(1-3 $_{\Delta B}$)-Fc protein bound more weakly still, and the Mut2: Flt1(2-3 $_{\Delta B}$)-Fc protein showed the best profile, binding more weakly than any of the other mutant proteins. The Mut4: Flt1(1-3 $_{R->N}$)-Fc glycosylation mutant protein showed only

25

marginal benefit on the Matrigel assay. These results confirm the hypothesis that a linear sequence of positive amino acids can be deleted from the primary sequence resulting in a decrease in charge interaction with extracellular matrix components.

5

(b.) Binding of Mut1: Flt1(1-3 $_{\Delta B}$)-Fc and Mut4: Flt1(1-3 $_{R->N}$)-Fc in a Biacore-based assay.

Unmodified and acetylated Flt1(1-3)-Fc and genetically modified Mut1: Flt1(1-3_{Δ B})-Fc and Mut4: Flt1(1-3_{R->N})-Fc proteins where tested in a Biacore-based assay to evaluate their ability to bind to the Flt1 ligand, VEGF. In this assay, unmodified Flt1(1-3)-Fc protein (0.25, 0.5, or 1.0 μ g/ml) was immobilized on the surface of a Biacore chip (see Biacore Instruction Manual, Pharmacia, Inc., Piscataway, NJ, for standard procedures) and a solution containing 0.1 μ g/ml VEGF and either purified or COS cell supernatant containing unmodified Flt1(1-3)-Fc (at approximately (0.25, 0.5, or 1.0 μ g/ml), purified acetylated Flt1(1-3)-Fc (at (0.25, 0.5, or 1.0 μ g/ml), COS cell supernatant containing Mut1: Flt1(1-3_{Δ B})-Fc (at approximately (0.25, 0.5, or 1.0 μ g/ml), or COS cell supernatant containing Mut4: Flt1(1-3_{R->N})-Fc (at approximately (0.25, 0.5, or 1.0 μ g/ml) were passed over the Flt1(1-3)-Fc-coated chip. As shown in Figure 17, at the sub-stoichiometric ratio (0.25 μ g/ml Flt1(1-3)-Fc of unmodified, acetylated or genetically modified samples vs. 01. μ g/ml VEGF), there is insufficient Flt1(1-3)-Fc protein to block binding of VEGF to the Flt1(1-3)-Fc immobilized on the Biacore chip.

5

At 0.5 μ g/ml of unmodified, acetylated or genetically modified Flt1(1-3)-Fc proteins, the stoichiometric ratio approximates 1:1 and there is an increased ability to block VEGF binding to the Biacore chip. At 1.0 μ g/ml of unmodified, acetylated or genetically modified Flt1(1-3)-Fc proteins, which is approximately a 10:1 stoichiometric ratio, the Flt1(1-3)-Fc proteins are able to block binding of VEGF to the Biacore chip, but they are not equivalent. Unmodified, acetylated, and Mut1: Flt1(1-3 $_{\Delta B}$)-Fc are essentially equal in their ability to block VEGF binding, whereas Mut4: Flt1(1-3 $_{R->N}$)-Fc is somewhat less efficient at blocking binding. These results confirm the hypothesis that it is possible to reduce the non-specific binding of a positively charged molecule by genetically removing a linear sequence of predominantly negatively charged amino acids.

(c.) Binding of Mut1: Flt1(1-3 $_{\Delta B}$)-Fc, Mut2: Flt1(2-3 $_{\Delta B}$)-Fc, Mut3: Flt1(2-3)-Fc, and in an ELISA-based assay.

To determine whether the three mutant proteins could bind the Flt1 ligand VEGF, binding experiments were done in which 96-well plates coated with VEGF were incubated with varying concentrations of the respective mutant protein, and after washing, the amount bound was detected by incubating with an alkaline phosphatase conjugated anti-human Fc antibody and quantitated colorimetrically by the addition of

an appropriate alkaline phosphatase substrate. As shown in Figure 19, this experiment showed that all the mutant proteins could bind VEGF similarly, at the concentrations tested.

5 Example 16: Pharmacokinetic analysis of acetylated Flt1(1-3)-Fc, Mut1: Flt1(1-3 $_{\Delta B}$)-Fc, and unmodified Flt1(1-3)-Fc.

In vivo experiments were designed to assess the pharmacokinetic profiles of unmodified Flt1(1-3)-Fc, Mut1: Flt1(1-3 $_{\Delta B}$)-Fc, and 40 fold molar excess acetylated Flt1(1-3)-Fc protein. Balb/c mice (25-30g) were injected subcutaneously with 4mg/kg of unmodified Flt1(1-3)-Fc, 40 fold molar excess acetylated Flt1(1-3)-Fc, and Mut1: Flt1(1-3 $_{\Delta B}$)-Fc proteins (4 mice each). These mice were tail bled at 1, 2, 4, 6, 24 hours, 2 days, 3 days, and 5 days after injection. The sera were assayed in an ELISA designed to detect Flt1(1-3)-Fc protein which involves coating an ELISA plate with VEGF, binding the Flt1(1-3)-Fc and reporting with an anti-Fc antibody linked to alkaline phosphatase. As shown in Figure 20, the Cmax for these reagents was as follows: Unmodified Flt1(1-3)-Fc - 0.15 μ g/ml; 40 fold molar excess acetylated Flt1(1-3)-Fc - 1.5 μ g/ml; and Mut1: Flt1(1-3 $_{\Delta B}$)-Fc - 0.7 μ g/ml.

Example 17: Modified Flt1 receptor vector construction

The rationale for constructing modified versions of the Flt1 receptor

(also known as VEGFR1) was based on the observation that the protein

25

5

sequence of Flt1 was highly basic, and was therefore likely to stick to extracellular matrix (ECM). The highly basic nature of Flt1 probably explains why unmodified Flt1(1-3)-Fc (described *supra*) has poor pharmacokinetics that make it difficult to use as a therapeutic agent. As described *supra*, the chemically modified form of 40 fold molar excess acetylated Flt1(1-3)-Fc, hereinafter termed A40, exhibited a greatly improved pharmacokinetic (PK) profile over the non-acetylated Flt1(1-3)-Fc. Therefore, attempts were made to engineer DNA molecules that could be used to recombinantly express modified forms of a Flt1 receptor molecule that would possess the improved PK profile exhibited by A40 and still maintain the ability to bind tightly to VEGF.

a net charge of +5 at neutral pH) is not essential for tight binding to VEGF, so this domain was deleted. The third Ig domain (having a net charge of +11) is not essential for binding, but confers higher affinity for VEGF than the second Ig domain, so instead of deleting it entirely, it was replaced with the equivalent domains of the Flt1 receptor relatives Flk1 (also known as VEGFR2) and Flt4 (also known as VEGFR3). These chimeric molecules (denoted R1R2 (Flt1.D2.Flk1D3.Fc Δ C1(a) and VEGFR1R2-Fc Δ C1(a) and R1R3 (Flt1D2.VEGFR3D3-Fc Δ C1(a) and VEGFR1R3-Fc Δ C1(a) respectively, wherein R1 and Flt1D2 = Ig domain 2 of Flt1 (VEGFR1); R2 and Flk1D3 = Ig domain 3 of Flk1 (VEGFR2); and R3 and VEGFR3D3 = Ig domain 3 of Flt4 (VEGFR3)) were much less sticky to ECM, as judged by an *in vitro* ECM binding assay as described *infra*, had

It is known in the literature that the first Ig domain of Flt1 (which has

greatly improved PK as described *infra*. In addition, these molecules were able to bind VEGF tightly as described *infra* and block phosphorylation of the native Flk1 receptor expressed in endothelial cells as described *infra*.

5

(a) Construction of the expression plasmid pFIt1D2.FIk1D3.Fc\(\Delta\)C1(a)

Expression plasmids pMT21.Flt1(1-3).Fc (6519bp) and pMT21.Flk-1(1-3).Fc (5230bp) are plasmids that encode ampicillin resistance and Fctagged versions of Ig domains 1-3 of human Flt1 and human Flk1, respectively. These plasmids were used to construct a DNA fragment consisting of a fusion of Ig domain 2 of Flt1 with Ig domain 3 of Flk1, using PCR amplification of the respective Ig domains followed by further rounds of PCR to achieve fusion of the two domains into a single fragment. For Ig domain 2 of Flt1, the 5' and 3' amplification primers were as follows:

5': bsp/flt1D2 (5'-GACTAGCAGTCCGGAGGTAGACCTTTCGTAGAGATG-3')

20

25

3': Flt1D2-Flk1D3.as (5'-CGGACTCAGAACCACATCTATGATTGTATTGGT-3')
The 5' amplification primer encodes a BspE1 restriction enzyme site
upstream of Ig domain 2 of Flt1, defined by the amino acid sequence
GRPFVEM (corresponding to amino acids 27-33 of Figure 21A-21C). The
3' primer encodes the reverse complement of the 3' end of Flt1 Ig

domain 2 fused directly to the 5' beginning of Flk1 Ig domain 3, with the fusion point defined as TIID of Flt1 (corresponding to amino acids 123-126 of Figure 21A-21C) and continuing into VVLS (corresponding to amino acids 127-130 of Figure 21A-21C) of Flk1.

5

For Ig domain 3 of Flk1, the 5' and 3' amplification primers were as follows:

5': Flt1D2-Flk1D3.s (5'-ACAATCATAGATGTGGTTCTGAGTCCGTCTCATG G-3')

3': Flk1D3/apa/srf.as (5'-GATAATGCCCGGGCCCTTTTCATGGACCCTGAC AAATG-3')

The 5' amplification primer encodes the end of Flt1 Ig domain 2 fused directly to the beginning of Flk1 Ig domain 3, as described above. The 3' amplification primer encodes the end of Flk1 lg domain 3, defined by the amino acids VRVHEK (corresponding to amino acids 223-228 of Figure 21A-21C), followed by a bridging sequence that includes a recognition sequence for the restriction enzyme Srf1, and encodes the amino acids GPG. The bridging sequence corresponds to amino acids 229-231 of Figure 21A-21C.

20

- 25

After a round of PCR amplification to produce the individual domains, the products were combined in a tube and subjected to a further round

25

5

of PCR with the primers bsp/flt1D2 and Flk1D3/apa/srf.as (described *supra*) to produce the fusion product. This PCR product was subsequently digested with the restriction enzymes BspEI and SmaI and the resulting 614bp fragment was subcloned into the BspEI to SrfI restriction sites of the vector pMT21/ΔB2.Fc, to create the plasmid pMT21/Flt1D2.Flk1D3.Fc. The nucleotide sequence of the Flt1D2-Flk1D3 gene fusion insert was verified by standard sequence analysis. This plasmid was then digested with the restriction enzymes EcoRI and SrfI and the resulting 702bp fragment was transferred into the EcoRI to SrfI restriction sites of the plasmid pFlt1(1-3)B2-FcΔC1(a) to produce the plasmid pFlt1D2.Flk1D3.FcΔC1(a). The complete DNA and deduced amino acid sequences of the Flt1D2.Flk1D3.FcΔC1(a) chimeric molecule is set forth in Figure 21A-21C.

(b) Construction of the expression plasmid pFIt1D2VEGFR3D3Fc△C1(a)

The expression plasmid pMT21.Flt1(1-3).Fc (6519bp) encodes ampicillin resistance and an Fc-tagged version of Ig domains 1-3 of human Flt1 receptor. This plasmid was used to produce a DNA fragment containing Ig domain 2 of Flt1 by PCR. RNA from the cell line HEL921.7 was used to produce Ig domain 3 of Flk1, using standard RT-PCR methodology. A further round of PCR amplification was used to achieve fusion of the two Ig domains into a single fused fragment. For Ig domain 2 of Flt1, the 5' and 3' amplification primers were as follows:

5': bsp/flt1D2 (5'-GACTAGCAGTCCGGAGGTAGACCTTTCGTAGAGATG-3')

5

The 5' amplification primer encodes a BspE1 restriction site upstream of Ig domain 2 of Flt1, defined by the amino acid sequence GRPFVEM (corresponding to amino acids 27-33 of Figure 22A-22C). The 3' amplification primer encodes the reverse complement of the end of Flt1 Ig domain 2 fused directly to the beginning of VEGFR3 Ig domain 3, with the fusion point defined as TIID of Flt1 (corresponding to amino acids 123-126 of Figure 22A-22C) and continuing into IQLL of VEGFR3 (corresponding to amino acids 127-130 of Figure 22A-22C).

For Ig domain 3 of VEGFR3, the 5' and 3' primers used for RT-PCR were as follows:

5': R3D3.s (ATCCAGCTGTTGCCCAGGAAGTCGCTGGAGCTGCTGGTA)

3': R3D3.as (ATTTTCATGCACAATGACCTCGGTGCTCTCCCGAAATCG)

20

Both the 5' and 3' amplification primers match the sequence of VEGFR3.

The 296bp amplification product of this RT-PCR reaction was isolated by standard techniques and subjected to a second round of PCR to add

suitable sequences to allow for fusion of the Flt1D2 with the Flk1D3 domains and fusion of the Flk1D3 and Fc domains via a GPG bridge (see below). The amplification primers were as follows:

- 5 5':Flt1D2.VEGFR3D3.s (TCATAGATATCCAGCTGTTGCCCAGGAAGTCGCTGGAG)
 - 3': VEGFR3D3/srf.as
 (GATAATGCCCGGGCCATTTTCATGCACAATGACCTCGGT)

The 5' amplification primer encodes the 3' end of Flt1 Ig domain 2 fused directly to the beginning (5' end) of VEGFR3 Ig domain 3, as described above. The 3' amplification primer encodes the 3' end of VEGFR3 Ig domain 3, defined by the amino acids VIVHEN (corresponding to amino acids 221-226 of Figure 22A-22C), followed by a bridging sequence that includes a recognition sequence for Srf1, and encodes the amino acids GPG. The bridging sequence corresponds to amino acids 227-229 of Figure 22A-22C.

After one round (for Flt1 Ig domain 2) or two rounds (for Flt4 Ig domain 3) of PCR to produce the individual Ig domains, the PCR products were combined in a tube and subjected to a further round of PCR amplification with the amplification primers bsp/flt1D2 and VEGFR3D3/srf.as described *supra*, to produce the fusion product. This PCR product was subsequently digested with the restriction enzymes

25

5

BspEI and Smal and the resulting 625bp fragment was subcloned into the BspEI to SrfI restriction sites of the vector pMT21/Flt1ΔB2.Fc (described *supra*), to create the plasmid pMT21/Flt1D2.VEGFR3D3.Fc. The sequence of the Flt1D2-VEGFR3D3 gene fusion insert was verified by standard sequence analysis. This plasmid was then digested with the restriction enzymes EcoRI and SrfI and the resulting 693bp fragment was subcloned into the EcoRI to SrfI restriction sites of the plasmid pFlt1(1-3)ΔB2-FcΔC1(a) to produce the plasmid designated pFlt1D2.VEGFR3D3.FcΔC1(a). The complete DNA deduced amino acid sequence of the Flt1D2.VEGFR3D3.FcΔC1(a) chimeric molecule is set forth in Figure 22A-22C.

Example 18: Extracellular Matrix Binding (ECM) Binding Assay

ECM-coated plates (Becton Dickinson catalog # 35-4607) were rehydrated with warm DME supplemented with glutamine (2mM), 100U penicillin, 100U streptomycin, and 10% BCS for at least 1 hr. before adding samples. The plates were then incubated for 1 hr. at room temperature with varying concentrations of Flt1D2.Flk1D3.FcΔC1(a) and Flt1D2.VEGFR3D3.FcΔC1(a) starting at 10nM with subsequent 2-fold dilutions in PBS plus 10% BCS. The plates were then washed 3 times with PBS plus 0.1% Triton-X and incubated with alkaline phosphatase-conjugated anti-human Fc antibody (Promega, 1:4000 in PBS plus 10% BCS) for 1 hr. at room temperature. The plates were then washed 4 times with PBS 0.1% Triton-X and alkaline phosphatase buffer/pNPP

25

5

solution (Sigma) was added for color development. Plates were read at I = 405-570nm. The results of this experiment are shown in Figure 23 and demonstrate that the Flt1D2.Flk1D3.FcΔC1(a) and Flt1D2.VEGFR3D3.FcΔC1(a) proteins are considerably less sticky to the ECM as compared to the Flt1(1-3)-Fc protein.

Example 19: Transient expression of pFlt1D2.Flk1D3.Fc∆C1(a) in CHO-K1 (E1A) cells

A large scale (2L) culture of E. coli DH10B cells carrying the pFlt1D2.Flk1D3.FcΔC1(a) plasmid described *supra* in Example 17(a) was grown overnight in Terrific Broth (TB) plus 100μg/ml ampicillin. The next day, the plasmid DNA was extracted using a QlAgen Endofree Megaprep kit following the manufacturer's protocol. The concentration of the purified plasmid DNA was determined by standard techniques using a UV spectrophotometer and fluorometer. The plasmid DNA was verified by standard restriction enzyme digestion of aliquots using the restriction enzymes EcoRl plus Notl and Asel. All restriction enzyme digest fragments corresponded to the predicted sizes when analyzed on a 1% agarose gel.

Forty 15 cm petri plates were seeded with CHO-K1/E1A cells at a density of 4 x 10⁶ cells/plate. Plating media was Gibco Ham's F-12 supplemented with 10% Hyclone Fetal Bovine Serum (FBS), 100U penicillin/100U streptomycin and glutamine (2mM). The following day

25

5

each plate of cells was transfected with 6 μg of the pFlt1D2.Flk1D3.FcΔC1(a) plasmid DNA using Gibco Optimem and Gibco Lipofectamine in 12 ml volume, following the manufacturer's protocol. Four hours after adding the transfection mix to the cells, 12 ml/plate of Optimem supplemented with 10% FBS was added. Plates were incubated at 37°C in a 5% CO₂ incubator overnight. The following day the media was removed from each plate and 25 ml expression media (Gibco CHO-S-SFM II supplemented with glutamine (2mM) and 1mM sodium butyrate) was added. The plates were incubated at 37°C for 3 days. After 3 days of incubation, the media was aspirated from each plate and centrifuged at 400 rpm in a swinging bucket rotor to pellet cells. The supernatant was decanted into sterile 1L bottles and purification of the expressed protein was performed as described *infra*.

Example 20: Construction pVEGFR1R2-Fc∆C1(a) expression vector

The pVEGFR1R2.FcΔC1(a) expression plasmid was constructed by insertion of DNA encoding amino acids SDT (corresponding to amino acids 27-29 of Figure 24A-24C) between Flt1d2-Flk1d3-FcΔC1(a) amino acids 26 and 27 of Figure 21A-21C (GG) and removal of DNA encoding amino acids GPG corresponding to amino acids 229-231 of Figure. The SDT amino acid sequence is native to the Flt1 receptor and was added back in to decrease the likelihood of heterogeneous N-terminal processing. The GPG (bridging sequence) was removed so that

the Flt1 and Flk1 Ig domains were fused directly to one another. The complete DNA and deduced amino acid sequences of the pVEGFR1R2.FcΔC1(a) chimeric molecule is set forth in Figure 24A-24C.

5 Example 21: Cell Culture Process Used to Produce Modified FIt1 Receptors

(a) Cell Culture Process Used to Produce FIt1D2.FIk1D3.Fc\(\Delta\)C1(a)

The process for production of Flt1D2.Flk1D3.FcΔC1(a) protein using the expression plasmid pFlt1D2.Flk1D3.FcΔC1(a) described *supra* in Example 1 involves suspension culture of recombinant Chinese hamster ovary (CHO K1/E1A) cells which constitutively express the protein product. The cells are grown in bioreactors and the protein product is isolated and purified by affinity and size exclusion chromatography. The process is provided in greater detail below.

Cell Expansion

20

25

Two confluent T-225 cm² flasks containing the Flt1D2.Flk1D3.Fc Δ C1(a) expressing cell line were expanded by passaging cells into eight T-225 cm² flasks in medium (GMEM + 10% serum, GIBCO) and incubated at 37°C and 5% CO2. When the flasks approached confluence (approximately 3 to 4 days) the cells were detached using trypsin. Fresh medium was added to protect the cells from further exposure to the trypsin. The cells

were centrifuged and resuspended in fresh medium then transferred to eight 850 cm² roller bottles and incubated at 37°C and 5% CO₂ until confluent.

5 Suspension Culture in Bioreactors

Cells grown in roller bottles were trypsinized to detach them from the surface and washed with suspension culture medium. The cells are aseptically transferred to a 5L bioreactor (New Brunswick Celligen Plus) where the cells are grown in 3.5L of suspension culture. The suspension culture medium was a glutamine-free low glucose modification of IS-CHO (Irvine Scientific) to which 5% fetal bovine serum (Hyclone), GS supplement (Life Technologies) and 25 μ M methionine sulfoximine (Sigma) was added. The pH was controlled at 7.2 by addition of carbon dioxide to the inlet gas or by addition of a liquid solution of sodium carbonate to the bioreactor. Dissolved oxygen level was maintained at 30% of saturation by addition of oxygen or nitrogen to the inlet gas and temperature controlled at 37°C. When a density of 4 x10⁶ cells/mL was reached the cells were transferred to a 40L bioreactor containing the same medium and setpoints for controlling the bioreactor. The temperature setpoint was reduced to 34°C to slow cell growth and increase the relative rate of protein expression.

20

5

(b) Cell Culture Process Used to Produce FIt1D2.VEGFR3D3.Fc△C1(a)

The same methodologies as described *supra* for Flt1D2.Flk1D3.FcΔC1(a) were used to produce Flt1D2.VEGFR3D3.FcΔC1(a).

Example 22: Harvest and Purification of Modified Flt1 Receptors

10 (a) Harvest and Purification of Flt1D2.Flk1D3.Fc∆C1(a)

The product protein was aseptically harvested from the bioreactor while retaining cells using Millipore Prostak tangential-flow filtration modules and a low-shear mechanical pump (Fristam). Fresh medium was added to the bioreactor to replace that removed during the harvest filtration. Approximately 40L of harvest filtrate was then loaded onto a 400 mL column containing Protein A Sepharose resin (Amersham Pharmacia). After loading the resin was washed with buffer containing 10 mM sodium phosphate, 500 mM sodium chloride, pH 7.2 to remove any unbound contaminating proteins. FIt1D2.FIk1D3.FcΔC1(a) protein was eluted with a pH 3.0 citrate buffer. The eluted protein was neutralized by addition of Tris base and frozen at -20°C.

Several frozen lots of Flt1D2.Flk1D3.Fc\(\Delta\C1(a)\) protein from the Protein 25 A step above were thawed, pooled and concentrated using a Millipore 30kD nominal molecular weight cutoff (NMWCO) tangential flow

25

5

filtration membrane. The protein was transferred to a stirred cell concentrator (Millipore) and further concentrated to 30 mg/mL using a 30kD NMWCO membrane. The concentrated protein was loaded onto a size exclusion column packed with Superdex 200 resin (Amersham Pharmacia) that was equilibrated with phosphate buffered saline plus 5% glycerol. The same buffer was used to run the column. The fractions corresponding to Flt1D2.Flk1D3.FcΔC1(a) dimer were pooled, sterile filtered through a 0.22 micron filter, aliquoted and frozen.

(b) Harvest and Purification of Flt1D2.VEGFR3D3.Fc∆C1(a)

The same methodologies as described *supra* for Flt1D2.Flk1D3.Fc∆C1(a) were used to harvest and purify Flt1D2.VEGFR3D3.Fc∆C1(a).

Example 23: Phosphorylation Assay for Transiently Expressed VEGFR2

Primary human umbilical vein endothelial cells (HUVECs), passage 4-6, were starved for 2 hrs in serum-free DME high glucose media. Samples containing 40 ng/ml (1nM) human VEGF165, which is a ligand for the VEGF receptors Flt1, Flk1 and Flt4(VEGFR3) were prepared and were preincubated for 1 hr. at room temperature with varying amounts of the modified Flt1 receptors Flt1(1-3)-Fc, Flt1(1-3)-Fc (A40),

Flt1D2Flk1D3.Fc\(\Delta\C1(a)\) and Flt1D2VEGFR3D3.Fc\(\Delta\C1(a)\) in serum-free DME-high glucose media containing 0.1% BSA. Cells were challenged for 5 minutes with the samples prepared above +/- VEGF165, followed by

whole cell lysis using complete lysis buffer. Cell lysates were immunoprecipitated with an antibody directed against the C-terminus of VEGFR2 receptor. The immunoprecipitated lysates were loaded onto 4-12% SDS-PAGE Novex gel and then transferred to PVDF membrane using standard transfer methodologies. Detection of phosphorylated VEGFR2 was done by immunoblotting with the anti-phospho Tyrosine mAb called 4G10 (UBI) and developed using ECL-reagent (Amersham). Figures 25A-25C and 26A-26B show the results of this experiment. Figure 25A-25C reveals that detection by Western blot of tyrosine phosphorylated VEGFR2(Flk1) by VEGF165 ligand stimulation shows that cell-surface receptors are phosphorylated to varying levels depending on which modified Flt1 receptor is used during the preincubations with VEGF. As is seen in Figure 25A, at a 1.5 molar excess of either Flt1(1-3)-Fc, Flt1(1-3)-Fc (A40) or transient Flt1D2Flk1D3.Fc∆C1(a) there is complete blockage of receptor stimulation by these three modified FIt1 receptors as compared to control media challenge. In contrast, transient Flt1D2VEGFR3D3.Fc△C1(a) does not show significant blockage at this molar excess, as compared with VEGF positive control challenge. Similar results are seen in Figure 25B, where the modified Flt receptors are in a 3-fold molar excess to VEGF165 ligand. In Figure 25C, where the modified Flt1 receptors are in a 6-fold molar excess to VEGF165 ligand, transient Flt1D2VEGFR3D3.Fc∆C1(a) can now be shown to be partially blocking VEGF165-induced stimulation of cell-surface receptors.

20

25

5

In Figure 26A-26B, detection by Western blot of tyrosine phosphorylated VEGFR2(Flk1) by VEGF165 ligand stimulation shows that cell-surface receptors are not phosphorylated by challenge samples which have VEGF165 preincubated with 1 and 2 fold molar excess (Figure 26A) or 3 and 4 fold molar excess (Figure 26B) of either transient Flt1D2Flk1D3.FcΔC1(a), stable Flt1D2Flk1D3.FcΔC1(a), or transient VEGFR1R2-FcΔC1(a). At all modified Flt1 receptor concentrations tested there is complete binding of VEGF165 ligand during the preincubation, resulting in no detectable stimulation of cell-surface receptors by unbound VEGF165 as compared to control media challenge.

Example 24: Cell Proliferation Bioassay

The test cell population is MG87 cells that have been stably transfected with a expression plasmid that contains a DNA insert encoding the VEGFR2(Flk1) extracellular domain fused to the TrkB intracellular kinase domain, thus producing a chimeric molecule. The reason the TrkB intracellular kinase domain was used rather than the native VEGFR2(Flk1) intracellular kinase domain is that the intracellular kinase domain of VEGFR2(Flk1) does not cause a strong proliferative response when stimulated by VEGF165 in these cells. It is known that MG87 cells containing full length TrkB receptor give a robust proliferative response when stimulated with BDNF, so the TrkB intracellular kinase domain was engineered to replace the intracellular

5

kinase domain of VEGFR2(Flk1) to take advantage of this proliferative response capability.

5 x 10³ cells/well were plated in a 96 well plate and allowed to settle for 2 hrs at 37°C. The following modified Flt receptors Flt1(1-3)-Fc, Flt1D2.Flk1D3.Fc∆C1(a) and Flt1D2.VEGFR3D3.Fc∆C1(a), plus an irrelevant receptor termed Tie2-Fc as a negative control, were titrated from 40nM to 20pM and incubated on the cells for 1hr at 37°C. Human recombinant VEGF165 in defined media was then added to all the wells at a concentration of 1.56nM. The plates were incubated for 72 hrs at 37°C and then MTS (Owen's reagent, Promega) added and the plates were incubated for an additional for 4 hrs. Finally, the plates were read on a spectrophotometer at 450/570nm. The results of this experiment are shown in Figure 27. The control receptor Tie2-Fc does not block VEGF165-induced cell proliferation at any concentration whereas Flt1D2.Flk1D3.Fc∆C1(a) blocks 1.56nM VEGF165 with a half maximal dose of 0.8nM. Flt1(1-3)-Fc and Flt1D2.VEGFR3D3.Fc∆C1(a) are less effective in blocking VEGF165 in this assay with a half maximal dose of ~ 2nM. VEGF165 alone gives a reading of 1.2 absorbance units and the background is 0.38 absorbance units.

Example 25: Binding Stoichiometry of Modified Flt Receptors to VEGF165

(a) BIAcore Analysis

5

The stoichiometry of Flt1D2Flk1D3.FcΔC1(a) and VEGFR1R2-FcΔC1(a) interaction with human VEGF165 was determined by measuring either the level of VEGF saturation binding to the Flt1D2Flk1D3.FcΔC1(a) or VEGFR1R2-FcΔC1(a) surfaces or measuring concentration of VEGF165 needed to completely prevent binding of Flt1D2Flk1D3.FcΔC1(a) or VEGFR1R2-FcΔC1(a) to VEGF BlAcore chip surface.

Modified Flt receptors Flt1D2Flk1D3.FcΔC1(a) and VEGFR1R2-FcΔC1(a), were captured with an anti-Fc specific antibody that was first immobilized on a Biacore chip (BIACORE) using amine-coupling chemistry. A blank antibody surface was used as a negative control. VEGF165 was injected at a concentration of 1 nM, 10 nM, and 50 nM over the Flt1D2Flk1D3.FcΔC1(a) and VEGFR1R2-FcΔC1(a) surfaces at 10 μl/min for one hour. A real-time binding signal was recorded and saturation binding was achieved at the end of each injection. Binding stoichiometry was calculated as a molar ratio of bound VEGF165 to the immobilized Flt1D2Flk1D3.FcΔC1(a) or VEGFR1R2-FcΔC1(a), using the conversion factor of 1000 RU equivalent to 1 ng/ml. The results indicated binding stoichiometry of one VEGF165 dimeric molecule per

5

one Flt1D2Flk1D3.FcΔC1(a) or VEGFR1R2-FcΔC1(a) molecule (Figure 28).

In solution, Flt1D2Flk1D3.Fc∆C1(a) or VEGFR1R2-Fc∆C1(a) at a concentration of 1nM (estimated to be 1000 times higher than the KD of the Flt1D2Flk1D3.Fc∆C1(a) or VEGFR1R2-Fc∆C1(a)/VEGF165 interaction) were mixed with varied concentrations of VEGF165. After one hour incubation, concentrations of the free Flt1D2Flk1D3.Fc∆C1(a) in solution were measured as a binding signal to an amine-coupled VEGF165 surface. A calibration curve was used to convert the Flt1D2Flk1D3.Fc\(\Delta\)C1(a) BIAcore binding signal to its molar concentration. The data showed that the addition of 1 nM VEGF165 into the Flt1D2Flk1D3.Fc\(\Delta\)C1(a) solution completely blocked Flt1D2Flk1D3.Fc\(\Delta\)C1(a) binding to the VEGF165 surface. This result suggested the binding stoichiometry of one VEGF165 molecule per one Flt1D2Flk1D3.Fc∆C1(a) molecule (Figure 29 and Figure 30). When the concentration of Flt1D2Flk1D3.Fc\(\Delta\)C1(a) was plotted as a function of added concentration of VEGF165, the slope of the linear portion was -1.06 for Flt1D2Flk1D3.Fc∆C1(a) and -1,07 for VEGFR1R2-Fc∆C1(a). The magnitude of the slope, very close to negative one, was indicative that one molecule of VEGF165 bound to one molecule of either Flt1D2Flk1D3.Fc Δ C1(a) or VEGFR1R2-Fc Δ C1(a).

(b) Size Exclusion Chromatography

Flt1D2Flk1D3.FcΔC1(a) was mixed with a 3-fold excess of VEGF165 and the receptor-ligand complex was purified using a Pharmacia Superose 6 size exclusion chromatography column. The receptor-ligand complex was then incubated in a buffer containing 6M guanidine hydrochloride in order to dissociate it into its component proteins.

Fit1D2Fik1D3.FcΔC1(a) was separated from VEGF165 using Superose 6 size exclusion chromatography column run in 6M guanidium chloride. In order to determine complex stoichiometry, several injections of Fit1D2Fik1D3.FcΔC1(a) and VEGF165 were made and peak height or peak integrated intensity was plotted as a function of the concentration of injected protein. The calibration was done under condition identical to one used in separating components of Fit1D2Fik1D3.FcΔC1(a)/VEGF complex. Quantification of the Fit1D2Fik1D3.FcΔC1(a)/VEGF complex composition was based on the calibration curves. The results of this experiment are set forth in Figure 28, which shows the ratio of VEGF165 to Fit1D2Fik1D3.FcΔC1(a) in a complex to be 1:1.

Example 26: Determination of the Binding Stoichiometry of FIt1D2FIk1D3.Fc∆C1(a)/VEGF165 Complex by Size Exclusion Chromatography

FIt1D2FIk1D3.Fc\(\Delta\)C1(a)/VEGF165 Complex Preparation

25

VEGF165 (concentration = 3.61 mg/ml) was mixed with CHO cell

transiently expressed Flt1D2.Flk1D3.Fc Δ C1(a) (concentration = 0.9 mg/ml) in molar ratio of 3:1 (VEGF165:Flt1D2.Flk1D3.Fc Δ C1(a)) and incubated overnight at 4°C.

5 (a) Size Exclusion Chromatography (SEC) under native conditions

To separate the complex from excess of unbound VEGF165, 50 μ l of the complex was loaded on a Pharmacia Superose 12 PC 3.2/30 which was equilibrated in PBS buffer. The sample was eluted with the same buffer at flow rate 40μ l/min. at room temperature. The results of this SEC are shown in Figure 31. Peak #1 represents the complex and peak #2 represents unbound VEGF165. Fractions eluted between 1.1 and 1.2 ml were combined and guanidinium hydrochloride (GuHCl)was added to a final concentration 4.5M to dissociate the complex.

25

5

(b) Siz Exclusion Chromatography (SEC) under dissociative conditions

To separate the components of the receptor-ligand complex and to determine their molar ratio, 50μ I of dissociated complex as described supra was loaded onto a Superose 12 PC 3.2/30 equilibrated in 6M GuHCl and eluted with the same solution at a flow rate 40μ I/min. at room temperature. The results of this SEC are shown in Figure 32. Peak #1 represents FIt1D2FIk1D3.Fc Δ C1(a) and peak #2 represents VEGF165.

(c) Calculation of Flt1D2Flk1D3.Fc\(\triangle C1(a)\):VEGF165 Complex Stoichiometry

The stoichiometry of the receptor-ligand complex was determined from the peak area or the peak height of the components. Concentrations of VEGF165 and Flt1D2Flk1D3.Fc Δ C1(a) corresponding to the peak height or peak area, respectively, were obtained from the standard curves for VEGF165 and Flt1D2Flk1D3.Fc Δ C1(a). To obtain a standard curve, four different concentrations (0.04 mg/ml -0.3mg/ml) of either component were injected onto a Pharmacia Superose 12 PC 3.2/30 column equilibrated in 6M guanidinium chloride and eluted with the same solution at flow rate 40μ l/min. at room temperature. The standard curve was obtained by plotting peak area or peak height vs protein concentration. The molar ratio of VEGF165:Flt1D2Flk1D3.Fc Δ C1(a) determined from the peak area of the components was 1.16. The molar

25

ratio of VEGF165:Flt1D2Flk1D3.Fc∆C1(a) determined from the peak height of the components was 1.10.

Example 27: Determination of the Stoichiometry of the

5 FIt1D2FIk1D3.Fc∆C1(a)/VEGF165 Complex by Size Exclusion

Chromatography with On-Line Light Scattering

Complex preparation

VEGF165 was mixed with CHO transiently expressed
Flt1D2.Flk1D3.FcΔC1(a) protein in molar ratio of 3:1
(VEGF165:Flt1D2Flk1D3.FcΔC1(a)) and incubated overnight at 4°C.

(a) Size Exclusion Chromatography (SEC) with On-Line Light Scattering

Size exclusion chromatography column with a MiniDawn on-line light scattering detector (Wyatt Technology, Santa Barbara, California) and refractive index (RI) detectors (Shimadzu, Kyoto, Japan) was used to determine the molecular weight (MW) of the receptor-ligand complex. Samples were injected onto a Superose 12 HR 10/30 column (Pharmacia) equilibrated in PBS buffer and eluted with the same buffer at flow rate 0.5 ml/min. at room temperature. As shown in Figure 33, the elution profile shows two peaks. Peak #1 represents the receptor-ligand complex and peak #2 represents the unbound VEGF165. MW was calculated from LS and RI signals. The same procedure was used to

5

determine MW of the individual components of the receptor-ligand complex. The results of these determinations are as follows: MW of the Flt1D2Flk1D3.FcΔC1(a)/VEGF165 complex at the peak position is 157 300 (Figure 33), the MW of VEGF165 at the peak position is 44 390 (Figure 34) and the MW of R1R2 at the peak is 113 300 (Figure 35).

These data indicated that the stoichiometry of the FIt1D2FIk1D3.FcΔC1(a)/VEGF complex is 1:1 as its corresponds to the sum of molecular weights for FIt1D2FIk1D3.FcΔC1(a) and VEGF165. Importantly, this method conclusively proved that the FIt1D2FIk1D3.FcΔC1(a)/VEGF165 complex was indeed composed of only one molecule of VEGF165 ligand and only one molecule of the FIt1D2FIk1D3.FcΔC1(a).

Example 28: Peptide Mapping of Flt1D2.Flk1D3.Fc\(\triangleC1(a)

The disulfide structures and glycosylation sites in Flt1D2.Flk1D3.Fc Δ C1(a) were determined by a peptide mapping method. In this method, the protein was first cleaved with trypsin. Tryptic fragments were analyzed and identified by HPLC coupled with mass spectrometry, in addition to an N-terminal sequencing technique. Reduction of the tryptic digest was employed to help identify disulfide-bond-containing fragments. Treatment of the tryptic digest with PNGase F (Glyko, Novato, CA) was employed to help identify

5

fragments with N-linked glycosylation sites. The results are summarized in the accompanying Figure 36.

There are a total of ten cysteines in Flt1D2.Flk1D3.Fc Δ C1(a); six of them belong to the Fc region. Cys27 has been confirmed to be disulfide bonded to Cys76. Cys121 is confirmed to be disulfide bonded to Cys 182. The first two cysteines in the Fc region (Cys211 and Cys214) form an intermolecular disulfide bond with the same two cysteines in another Fc chain. However, because these two cysteines can not be separated enzymatically from each other, it can not be determined whether disulfide bonding is occurring between same cysteines (Cys211 to Cys211, for example) or between Cys211 and Cys214. Cys216 is confirmed to be disulfide bonded to Cys306. Cys 352 is confirmed to be disulfide bonded to Cys410.

There are five possible N-linked glycosylation sites in Flt1D2.Flk1D3.Fc Δ C1(a). All five of them are found to be glycosylated to varying degrees. Complete glycosylation was observed at Asn33 (amino acid sequence NIT), Asn193 (amino acid sequence NST), and Asn282 (amino acid sequence NST). In addition, partial glycosylation isobserved on Asn65 and Asn120. Sites of glycosylation are highlighted by underline in the Figure 36.

Example 29: Pharmacokinetic Analysis of Modified Flt Receptors

(a) Pharmacokinetic analysis of Flt1(1-3)-Fc (A40), 5 Flt1D2.Flk1D3.Fc△C1(a) and VEGFR1R2-Fc△C1(a)

Balb/c mice (25-30g) were injected subcutaneously with 4mg/kg of Flt1(1-3)-Fc (A40), CHO transiently expressed Flt1D2.Flk1D3.Fc∆C1(a), CHO stably expressed Flt1D2.Flk1D3.Fc△C1(a), and CHO transiently expressed VEGFR1R2-Fc∆C1(a). The mice were tail bled at 1, 2, 4, 6, 24hrs, 2 days, 3 days and 6 days after injection. The sera were assayed in an ELISA designed to detect Flt1(1-3)-Fc (A40), Flt1D2.Flk1D3.FcΔC1(a) or VEGFR1R2-FcΔC1(a). The ELISA involves coating an ELISA plate with VEGF165, binding the detect Flt1(1-3)-Fc (A40), Flt1D2.Flk1D3.Fc∆C1(a) or VEGFR1R2-Fc∆C1(a) and reporting with an anti-Fc antibody linked to horse radish peroxidase. The results of this experiments are shown in Figure 37. The T_{max} for Flt1(1-3)-Fc (A40) was at 6 hrs while the T_{max} for the transient and stable Flt1D2.Flk1D3.Fc∆C1(a) and the transient VEGFR1R2-Fc∆C1(a) was 24hrs. The C_{max} for Flt1(1-3)-Fc (A40) was $8\mu g/ml$. For both transients (Flt1D2.Flk1D3.Fc∆C1(a) and VEGFR1R2-Fc∆C1(a)) the C_{max} was 18µg/ml and the C_{max} for the stable VEGFR1R2-Fc∆C1(a) was $30\mu g/mI$.

20

25

5

(b) Pharmacokinetic analysis of Flt1(1-3)-Fc (A40), Flt1D2.Flk1D3.Fc\(\Delta\)C1(a) and Flt1D2.VEGFR3D3.Fc\(\Delta\)C1(a)

Balb/c mice (25-30g) were injected subcutaneously with 4mg/kg of Flt1(1-3)-Fc (A40), CHO transiently expressed Flt1D2.Flk1D3.FcΔC1(a) and CHO transiently expressed Flt1D2.VEGFR3D3.FcΔC1(a). The mice were tail bled at 1, 2, 5, 6, 7, 8, 12, 15 and 20 days after injection. The sera were assayed in an ELISA designed to detect Flt1(1-3)-Fc, Flt1D2.Flk1D3.FcΔC1(a) and Flt1D2.VEGFR3D3.FcΔC1(a). The ELISA involves coating an ELISA plate with 165, binding the Flt1(1-3)-Fc, Flt1D2.Flk1D3.FcΔC1(a) or Flt1D2.VEGFR3D3.FcΔC1(a) and reporting with an anti-Fc antibody linked to horse radish peroxidase. Flt1(1-3)-Fc (A40) could no longer be detected in the serum after day 5 whereas , Flt1D2.Flk1D3.FcΔC1(a) and Flt1D2.VEGFR3D3.FcΔC1(a) were detectable for 15 days or more. The results of this experiment are shown in Figure 38.

Example 30: Evaluation of the Ability of FIt1D2.FIk1D3.Fc\(\triangle C1(a)\) to Inhibit Tumor Growth In Vivo

To evaluate the ability of Flt1D2.Flk1D3.FcΔC1(a) to inhibit tumor growth in vivo a model in which tumor cell suspensions are implanted subcutaneously on the right flank of male severe combined immunodeficiency (SCID) mice was employed. Two cell lines, the human HT-1080 fibrosarcoma cell line (ATCC accession no. CCL-121) and the rat C6 glioma cell line (ATCC accession no. CCL-107), each of

5

which exhibit distinctly different morphologies and growth characteristics, were used in the assay. The first dose of Flt1D2.Flk1D3.FcΔC1(a) (at 25mg/Kg or as indicated in Figures 39 and 40) was given on the day of tumor implantation. Animals subsequently received subcutaneous injections of Flt1(1-3)-Fc (A40), Flt1D2.Flk1D3.FcΔC1(a) or vehicle either every other day (EOD) or two times per week (2X/wk) for a period of 2 weeks. After 2 weeks, animals were perfused with fixative, tumors were removed and samples were blinded. Tumor volume was determined by measuring the length and width of visible subcutaneous tumors. Both of Flt1(1-3)-Fc (A40) and Flt1D2.Flk1D3.FcΔC1(a) significantly reduced the growth of tumors formed by HT-1080 and C6 cells. The results of these experiments are shown in Figure 39 and Figure 40.

Example 31: The Effect of VEGF165 and Modified Flt Receptors in Female Reproductive System

The stereotypic pattern of vascular remodeling which occur in the uterus and ovary over the course of the reproductive cycle has been well characterized, making these tissues particularly well suited to the study of mechanisms which regulate angiogenesis, vascular remodeling and vascular regression. Indeed, *in situ* hybridization studies in the reproductive tissues provided the first clear evidence

5

that VEGF acts as a mediator of physiological angiogenesis in mature rodents, as well as humans and non-human primates (Phillips et al, 1990; Ravindranath et al, 1992; Shweiki et al, 1993; Kamat et al, 1995). As cyclic angiogenesis and vascular remodeling are prominent features of the normal ovary and uterus, it is not surprising that abnormal blood vessel growth and/or vascular dysfunction have been found to characterize many pathological conditions which affect these organs. Furthermore, these pathogenic vascular abnormalities are thought to be caused or perpetuated by the dysregulated expression of one or more angiogenic or anti-angiogenic factors, most prominently VEGF.

For example, abnormal angiogenesis is characteristic of polycystic ovary disease, endometriosis and endometrial carcinoma, and in each case VEGF is over expressed in the affected tissue (Kamat et al, 1995; Shifren et al, 1996; Guidi et al, 1996; Donnez et al, 1998).

Overexpression of VEGF is also thought to play a pathogenic role in the establishment of systemic vascular hyperpermeability in ovarian

5

hyperstimulation syndrome (McClure et al, 1994; Levin et al, 1998) and preeclampsia (Baker et al, 1995; Sharkey et al, 1996). In addition, VEGF has been implicated as the permeability factor responsible for the production of ascites associated with ovarian carcinoma and other tumors (Senger et al, 1983; Boocock et al, 1995). Agents which effectively neutralize the biological actions of VEGF can reasonably be anticipated to be of therapeutic benefit in the above and related conditions.

Angiogenesis and vascular remodeling are also hallmarks of blastocyst implantation and placental development (Findlay, 1986). VEGF is strongly expressed both in the maternal decidua and in embryonic trophoblasts, where it is thought to first stimulate expansion and hyperpermeability of the uterine vasculature during the perimplantation period and subsequently mediate formation of both the maternal and embryonic components of the placental vasculature (Shweiki et al, 1993; Cullinan-Bove and Koos, 1993; Chakraborty et al, 1995; Das et al, 1997). VEGF is also required for luteal angiogenesis

5

and associated progesterone secretion necessary to prepare the uterus for implantation (Ferrara et al, 1998). Thus, agents which inhibit the biological actions of VEGF may prove to be useful as contraceptive agents (by preventing implantation), or as an abortifacients in the early stages of gestation. The latter application might find particular use as a non-surgical intervention for the termination of ectopic pregnancies.

While the expression of VEGF receptors is largely confined to the vascular endothelium in normal reproductive tissues, Flt1 is also expressed by trophoblasts in the placenta in both humans and animals (Clark et al, 1996; He et al, 1999) where it has been proposed to play a role in trophoblast invasion. Interestingly, both Flt1 and KDR (Flk1) are expressed by choriocarcinoma cell line BeWo (Charnock-Jones et al, 1994), and VEGF has been shown to promote DNA synthesis and tyrosine phosphorylation of MAP kinase in these cells. Furthermore, primary and metastatic ovarian carcinomas not only to express high levels of VEGF, but - in addition to the vascular endothelium - the tumor cells themselves express KDR and/ or Flt1 (Boocock et al, 1995). These

20

5

findings suggest that VEGF may not only be critically involved in the generation and maintenance of tumor vasculature, but that at least in some tumors of reproductive origin VEGF may subserve an autocrine role, directly supporting the survival and proliferation of the tumor cells. Thus agents which block the actions of VEGF may have particularly beneficial applications to the treatment of tumors of reproductive origin.

Methods and Results

(a) Assessment of VEGF-Induced Uterine Hyperpermeability

Pregnant mare's serum gonadotrophin (PMSG) was injected subcutaneously (5 IU) to induce ovulation in prepubertal female rats. This results in a surge of estradiol after 2 days which in turn causes an induction of VEGF in the uterus. It is reported that this induction results in hyperpermeability of the uterus and an increase in uterine wet weight 6 hrs. later and, therefore, could potentially be blocked by the modified Flt receptors Flt1(1-3)-Fc (A40), Flt1D2.Flk1D3.FcΔC1(a) and Flt1D2.VEGFR3D3.FcΔC1(a). In this in vivo model, the normal weight of the rat uterus is about 50 mg and this can be induced to 300-350 mg by PMSG. Desiccation of the tissue reveals that this is all

25

5

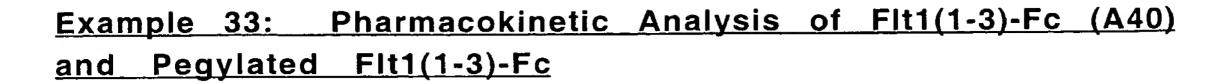
water weight. Subcutaneous injection of Flt1(1-3)-Fc (A40), Flt1D2.Flk1D3.FcΔC1(a) and Flt1D2.VEGFR3D3.FcΔC1(a) at 25mg/kg at 1hr. after PMSG injection results in about a 50% inhibition of the increase in uterine wet weight. Increasing the dose of modified Flt receptor does not further reduce the increase in wet weight suggesting that there is a VEGF-independent component to this model. The results of this experiment are shown in Figure 41.

(a) Assessment of corpus luteum angiogenesis using progesterone as a readout

Pregnant mare's serum gonadotrophin (PMSG) is injected subcutaneously (5 IU) to induce ovulation in prepubertal female rats. This results in a fully functioning corpus luteum containing a dense network of blood vessels after 4 days that allows for the secretion of progesterone into the blood stream in order to prepare the uterus for implantation. The induction of angiogenesis in the corpus luteum requires VEGF; therefore, blocking VEGF would result in a lack of new blood vessels and thus a lack of progesterone secreted into the blood stream. In this in vivo model, resting levels of progesterone are about 5ng/ml and this can be induced to a level of 25-40ng/ml after PMSG. Subcutaneous injection of Flt1(1-3)-Fc (A40) or Flt1D2.Flk1D3.FcΔC1(a) at 25mg/kg or 5mg/kg at 1hr. after PMSG injection results in a complete inhibition of the progesterone induction on day 4. The results of this experiment are shown in Figure 42A-42B.

25

5



Flt1(1-3)-Fc was PEGylated with either 10kD PEG or 20kD PEG and tested in balb/c mice for their pharmacokinetic profile. Both PEGylated forms of Flt1(1-3)-Fc were found to have much better PK profiles than Flt1(1-3)-Fc (A40), with the Tmax occurring at 24 hrs. for the PEGylated molecules as opposed to 6 hrs. for Flt1(1-3)-Fc (A40).

Example 34: VEGF165 ELISA to Test Affinity of Modified Flt1 Receptor Variants

10pM of VEGF165 was incubated overnight at room temperature with modified Flt1 receptor variants ranging from 160pM to 0.1pM. The modified Flt1 receptor variants used in this experiment were Flt1(1-3)-Fc, Flt1(1-3)-Fc (A40), transiently expressed Flt1D2VEFGFR3D3-Fc Δ C1(a), transiently expressed Flt1D2VEFGFR3D3-Fc Δ C1(a), Flt1-(1-3 $_{NAS}$)-Fc, Flt1(1-3 $_{R->C}$)-Fc and Tie2-Fc. Flt1(1-3 NAS)-Fc is a modified version of Flt1(1-3)-Fc in which the highly basic amino acid sequence KNKRASVRRR is replaced by NASVNGSR, resulting in the incorporation of two new glycosylation sites and a net reduction of five positive charges, both with the purpose of reducing the unfavorable effects of this sequence on PK. Flt1(1-3 $_{R->C}$)-Fc is a modification in which a single arginine (R) residue within the same basic amino acid sequence is changed to a cysteine (C) (KNKRASVRRR -> KNKCASVRRR) to allow for pegylation at that residue, which could then

25

5

shield the basic region from exerting its unfavorable effects on PK. After incubation the solution was transferred to a plate containing a capture antibody for VEGF165 (R&D). The amount of free VEGF165 was then determined using an antibody to report free VEGF165. This showed that the modified Flt1 receptor variant with the highest affinity for VEGF165 (determined as the lowest amount of free VEGF165) was Flt1D2Flk1D3.Fc Δ C1(a), followed by Flt1(1-3)-Fc and Flt1(1-3)-Fc (A40) and then by Flt1(1-3_{R->C})-Fc, Flt1(1-3_{NAS})-Fc and Flt1D2VEFGFR3D3-Fc Δ C1(a). Tie2Fc has no affinity for VEGF165.

Example 35: The effects of VEGFR1R2-Fc \(C1(a) \) in a novel animal model of psoriasis.

Introduction

Psoriasis is a chronic skin disease characterized by red patches that are covered with white scales and is often accompanied by varying degrees of discomfort. The disease is not contagious; however, its cause and mechanism have not yet been determined. Because of the formation of unsightly skin lesions and eruptions, psoriasis often has a negative psychological impact on its sufferers. Among people in Western countries, approximately 2-3% of the total population suffers from the disease. Various classifications have been proposed for psoriasis, but it is generally classified into psoriasis vulgaris, pustular psoriasis, psoriatic arthritis, guttate psoriasis, and the like.

25

5

Of these, psoriasis vulgaris is the major type and accounts for 80 to 90% of all instances of the disease.

Psoriasis is considered to be a multicausal hereditary disease which is often triggered by the action of various non-genetic factors such as injury, infection, drugs, food, climate, and stress. Furthermore, psoriasis is known to be associated with certain histocompatibility antigens (HLA). In fact, studies have linked certain types of psoriasis with specific HLAs. For example, Tiilikainen, A., et al, (Br J Dermatol, 1980 102:179-84) have reported that the prevalence of histocompatibility antigen HLA-Cw6 is 72.7% in twenty-two patients with the guttate form of psoriasis and 45.9% in thirty-seven patients with the vulgaris form of psoriasis. Thus, psoriasis clearly is a disease with a genetic basis in its cause.

There are two characteristic symptoms of psoriasis including 1) an inflammatory response common to that caused by other superficial skin diseases and 2) a tendency toward abnormal growth of the cuticle of the skin. The inflammatory response is characterized by vascular permeability, T-lymphocyte hypermigration, and release of the T-helper type I (THI) cytokine into the epidermis (Nickoloff, BJ, 1999, Arch Dermatol Sep;135(9):1104-10). The abnormal cuticle growth is characterized by epidermal acanthosis and rete ridge formation in more mature psoriasis. In more advanced psoriatic lesions, confluent parakeratosis with aberrantly differentiated keratinocytes containing

25

5

nuclei in stratum corneum and microabcesses with neutrophils arranged in tiers within the confluent parakeratotic cornified layer (Altman E and Kamino H., 1999, Seminars in Cutaneous Medicine and Surgery 18:25-35) often develop. These are the key features for the clinical diagnosis of psoriasis.

The therapeutic methods currently available to treat psoriasis include the control of the hyperproliferation of epidermal cells; control of the inflammatory response; promotion of immunomodulation; and avoidance of infection by bacteria and fungi. The following is a summary of the therapeutic methods that are generally utilized: (1) External and internal use of adrenocortical hormone - The external or topical use of a steroid has the immediate effect of reducing the symptoms of psoriasis, particularly the reduction of eruptions. However, administration of adrenocortical hormone over long periods of time increases resistance and tolerance buildup, so that the dose must be increased, or stronger drugs must be used, in order to obtain an acceptable therapeutic effect. In addition, when the psoriatic lesion occurs over a relatively large area, it cannot be completely cured by this method alone and, therefore, must be combined with other therapies; (2) Photochemotherapy - This method consists of administering psoralen in the form of an external or internal preparation and applying longwave ultraviolet rays to the affected region. Unfortunately, not all types of psoriasis can be treated by this method; (3) Phototherapy (UV Irradiation) - While this mode of

25

5

treatment is often effective, over time it has the undesirable side effect of causing accelerated aging of the skin. In addition, there is the risk of inducing carcinogenesis; (4) External use of coal tar - Coal tar suppresses the growth of cells so that the psoriatic lesion diminishes over a short period of time and a relatively long remission period may be achieved. However, occasionally, other skin disorders can result such as stimulant dermatitis and folliculitis (tar acne); (5) Administration of methotrexate - Methotrexate is an antagonist against folic acid, which is active in inhibiting the growth of cells. The use of methotrexate is effective for treating pustular psoriasis. Unfortunately, the use of methotrexate for a long period of time causes adverse effects such as disturbances in liver function, suppression of myeloproliferation, and loss of reproductive function; (6) Administration of retinoid - Retinoid is considered to have an immunomodulation effect in that it may control the abnormal cornification of epidermal cells and increased leukocyte migration. The internal administration of retinoid-based therapeutics is particularly effective for treating pustular psoriasis and psoriatic erythroderma. However, retinoid can exhibit adverse effects such as a decrease in the thickness of the skin and the visible mucous membranes. Furthermore, abnormal levels of serum lipoprotein are occasionally observed. Importantly, because retinoid is teratogenic and likely to accumulate and remain inside the body for a long period of time, the administration of retinoid to people of childbearing age is avoided, thus limiting the patient population to those who are beyond childbearing age or who are

25

5

suffering from intractable psoriasis; and (7) Cyclosporin A - an immunosuppressant that is often used by physicians for treating psoriasis. The major disadvantage of cyclosporin A as a treatment for psoriasis is that it is a general immunosuppressant, thus making patients more vulnerable to infection or other bacterial or viral diseases.

Recent studies have shown that the growth factor VEGF is upregulated in psoriatic lesions (Detmar M, et al., 1994, J Exp Med 1;180(3):1141-6.) However, to date there are no data that describe what role the overexpression of VEGF may have in either the development of or the progression of psoriasis. It is known that VEGF causes vascular permeability, increased microvascular density and enhanced leukocyte rolling and adhesion (Detmar M, et al., 1998, J Invest Dermatol 1998 Jul;111(1):1-6). Increased expression of VEGF has also been identified in chronic inflammatory dermatoses, including Bullous Pemphigoid, dermatitis herpetiformis, and erythema multiforme, all of which are characterized by hyperpermeable dermal microvessels and pronounced papillary dermal edema (Brown LF, et al., 1995, J Invest Dermatol 104(5):744-9).

While there are therapies available to treat psoriasis, most of these available therapies are less than ideal due to the severity of their side effects, the eventual development of resistance, and/or limitations on suitable patient populations, thus rendering clear the need for new safe

and effective treatments for psoriasis. To satisfy this need,

Applicants have discovered a new and novel method of treating

psoriasis, such method utilizing a novel protein molecule that is able to

reverse psoriatic-like lesions in a relatively short period of time with

no apparent side effects during the course of treatment.

Applicants have also developed a new, novel, and reliable animal model for clinical psoriasis, thus making it easier to study and understand the underlying mechanisms of the disease, as well aiding in the search for new therapies.

Materials and Methods

A. K14VEGF Transgenic mice

A Keratin-14 (K14)-based expression vector and a mouse cDNA encoding VEGF164 was used to generate K14VEGF transgenic mice by an approach identical to that used for generating K14-Ang1 mice (Suri C, et al., 1998. Science 16;282(5388):468-71). The K14 promoter directs expression of VEGF to the basal layer of the epidermis, including cells lining the hair (Suri C, et al., 1998. Science 16;282(5388):468-71). The K14VEGF transgenic homozygous mice were used throughout the studies described herein.

5

B. Tissue processing and immunostaining

For immunohistochemistry, 10µm cryo-sections of ear skin obtained from both wild-type and K14VEGF transgenic mice were stained with anti-mouse platelet-endothelial cell adhesion molecule-1 (PECAM-1, CD31, PharMingen, San Diego, CA), anti-mouse CD4 (BD PharMingen, San Diego, CA), CD8 (BD PharMingen, San Diego, CA), anti-mouse F4/80 (Serotec, Oxford, England), or anti-mouse VEGF (R&D systems, Minneapolis, MN). For immunostaining with PECAM-1 and VEGF, tissue sections were pre-fixed in 4% paraformaldehyde before staining according to standard procedure known in the art. For immunostaining with CD4, CD8, or F4/80 antibody, acetone-fixed tissue sections were used that were prepared by standard techniques familiar in the art.

C. Histology

Hematoxolin and eosin (H&E) staining were performed according to standard protocols familiar to the skilled artisan.

20 D. VEGFR1R2-Fc∆C1(a) injection

The K14VEGF homozygous transgenic mice were treated with VEGFR1R2-Fc∆C1(a) by subcutaneous injection into the neck skin. The mice were treated with either 25 mg/kg VEGFR1R2-Fc∆C1(a) or 12.5 mg/kg human Fc as a control, using an injection schedule of every three

days for 10 days resulting in a total of four injections per animal.

Photographs of the mice were taken immediately before each injection.

Mouse ear tissue was harvested on day 12 for subsequent histological analyses.

5

Results

A. Phenotype of K14VEGF transgenic mice

As previously reported, the K14VEGF transgenic mice are fertile and overtly healthy (Suri C, et al., 1998. Science 16;282(5388):468-71; Detmar M, et al., 1998, J Invest Dermatol 1998 Jul;111(1):1-6). However, the ear skin of the K14VEGF transgenic mice is visibly redder than that of their wild-type FVB littermates. Focal lesions which appeared similar to psoriatic lesions started to develop on the ear skin and, to a lesser extent, on the dorsal and lateral skin of young K14VEGF transgenic mice. The condition worsened with age. Massive skin lesions were observed on the ears of these transgenic mice by age 5 months or older. Lesions were accompanied by bloody, flaky skin, and hair loss. Figure 43 is a photograph of the mice exhibiting such massive lesions at about 6 months of age.

25

5

B. Expression of VEGF in th skin of K14VEGF transgenic mice

VEGF transgene expression was detected by immunostaining with an antibody specific to mouse VEGF. Strong protein expression was observed in basal keratinocytes and in microvessels in the papillary dermis.

C. <u>Histological analyses of psoriatic lesions in K14VEGF</u> transgenic <u>mice</u>

Histological analyses of K14VEGF transgenic mouse ears exhibiting the psoriatic lesions revealed a characteristic psoriatic skin phenotype. Standard hematoxolin and eosin (H&E) staining revealed that the epidermis of young K14VEGF transgenic mice exhibited moderate acanthosis (i.e. epidermal hyperplasia) and focal parakeratosis (i.e. keratinocytes in the stratum corneum retain nuclei) compared to control mouse (see Figure 44A and 44B). In the dermal compartment, edema coupled with an approximately 5-fold increase in tissue thickness was observed, as was inflammatory cell infiltration. The condition progressed with age. K14VEGF transgenics over 6 months of age developed obvious rete ridges that are typical for psoriasiform hyperplasia and the skin became more thickened (see Figure 45). More confluent hyperkeratosis with excessive deposition of keratin, and parakeratosis with neutrophil-laden pustules were present in the stratum corneum (Figure 44C). Munro microabscesses (Figure 46A)

25

5

localized within parakeratotic areas of the cornified layer (Altman, E. and Kamino, H., 1999, Seminars in Cutaneous Medicine and Surgery 18:25-35) and Kogoj (Altman, E. and Kamino, H., 1999, Seminars in Cutaneous Medicine and Surgery 18:25-35) microabscesses (Figure 46B) that localized immediately beneath the parakeratotic cornified layer were identified in the lesions of older K14VEGF transgenics. The presence of microabscesses are key features in clinical psoriasis diagnosis (Altman, E. and Kamino, H., 1999, Seminars in Cutaneous Medicine and Surgery 18:25-35).

K14VEGF transgenic mice are characterized by visible skin redness and vascularization. Immunohistological staining for PECAM-1, an integral membrane protein located on endothelial cells (DeLisser, HM, et al., 1994, Immunol Today Oct;15(10):490-5), revealed an increased number of dermal microvessels within K14VEGF transgenic skin. Dilated and tortuous capillaries in the papillary dermis, that spiral to near the undersurface of the epidermis, were also observed.

The pathological basis for psoriasis is not known. One issue is whether the disorder reflects an abnormality in the epidermal keratinocyte or bone-marrow-derived immunocytes. Recent studies using severe combined immunodeficient (SCID) mice engrafted with symptomless skin from a psoriasis patient provided direct in vivo evidence that activated CD4+, but not CD8+ T-lymphocytes, can trigger the formation of a psoriatic phenotype (Wrone-Smith, T, Nickoloff, BJ, 1996, J Clin

5

Invest 1996 Oct 15;98(8):1878-87; Nickoloff, BJ, Wrone-Smith ,T., 1999, Am J Pathol 1999 Jul;155(1):145-58)To analyze the immunologic basis that mediates the inflammatory response in the K14VEGF transgenic mouse psoriasis model described herein, immunostaining was performed for CD4+ and CD8+ immunocytes. The results revealed massive infiltration of CD4+ T-lymphocytes that are localized primarily in the dermis of both early psoriatic lesions and in more mature psoriatic lesions isolated from older K14VEGF transgenic mice. The overall level of CD8+ T-lymphocytes that infiltrated into the lesional skin was significantly less than that of the CD4+ Tlymphocytes. In young K14VEGF transgenic lesions, CD8+ Tlymphocytes were detected in both the dermis and the epidermis. Interestingly, CD8+ lymphocytes become primarily localized in the epidermis with maturation of psoriatic lesion. When cryosections of skin from K14VEGF transgenic mice were stained with an antibody recognizing the murine macrophage marker F4/80 antigen, a significant increase in the number of macrophages was observed as compared to control. This increased macrophage infiltration became even more dramatic with the development of psoriatic lesions in older transgenic mice, which suggests that the cytokines or growth factors secreted by activated CD8+ lymphocytes further stimulate macrophage proliferation leading to exacerbation of psoriatic phenotype.

5

G. The effects of VEGFR1R2-Fc△C1(a) in an animal model of psoriasis

The novel animal model of psoriasis described herein demonstrates that a psoriatic phenotype can be induced primarily by over expression of VEGF in the mouse epidermis. To confirm the causative role of VEGF in the formation of a psoriatic lesion, VEGFR1R2-Fc∆C1(a) was injected subcutaneously into mouse neck skin. VEGFR1R2-Fc∆C1(a) competes with endogenous mouse VEGF receptor for binding of VEGF by forming a complex with the VEGF, thus preventing it from binding to its receptor and transducing a signal. Five K14VEGF transgenic mice with obvious psoriatic lesions were treated on days 0 (Fig. 47A-47D), day 3 (Fig. 47E-47H), day 7 (Fig. 47I-47L), and day 10 (Fig. 47M-47P), with VEGFR1R2-Fc∆C1(a) at a dose of 25 mg/kg. Three of the treated mice showed significant improvement of the skin lesions by day 3, following the first injection of VEGFR1R2-Fc\(\Delta\)C1(a). The remaining two of the animals showed mild improvement in their lesions by day 3. Subsequent injections of VEGFR1R2-Fc\(\Delta\)C1(a) demonstrated further improvements in the skin lesions in all the mice up to day 7. However, by day 10, two of the mice started to develop small focal lesions, presumably due to the formation of VEGFR1R2-Fc\(\Delta\)C1(a) neutralizing antibodies (Figure 47A-47P).

Example 36: The effects of VEGFR1R2-Fc (a) in a nov lanimal model of wound healing

Introduction

5

During the early phase of wound healing, new granulation tissue begins to form approximately 4 days after the injury. Numerous new capillaries along with fibroblasts and extracellular matrix proteins move into the wound space (Hunt TK, 1980, World J Surg 4(3):271-7). Neo-vascularization provides oxygen and nutrients necessary to sustain cell metabolism. In fact, adequate new blood vessel formation seems to be crucial to the normal process of wound healing. However, the growth factor(s) that stimulate the angiogenesis associated with wound healing as well as the underlying molecular mechanisms at play remain elusive.

VEGF, a potent angiogenesis factor, has strong vasopermeability activity (Dvorak HF, et. al., 1995, Am J Pathol 146(5):1029-39) and is produced in large quantities by the epidermis during wound healing (Brown LF, et. al., 1992, J Exp Med1;176(5):1375-9). Therefore, Applicants decided to study the potential role of VEGF in wound healing using Applicants' novel murine excisional wound healing model.

25

5

Methods

A. Murine excisional wound healing model

A novel wound healing model was created by introducing an excisional wound on the dorsal skin of a mouse ear. Female FVB mice (Taconic, NY) weighing approximately 25 to 30g were used in this experiment. Animals were housed under standard conditions, and provided food and Post-operatively, animals were housed in individual water ad libitum. cages under standard conditions, and checked daily for signs of healing. Mice were anesthetized using ketamine (200 mg/kg) and xylazine (10 mg/kg) through intraperitoneal injection. Using electric clippers, the hair on the ear skin of the mice was gently shaved. A standard depilating agent was applied to remove the remaining hair, and PBS and betadine was used to clean the exposed skin. One full-thickness, circular wound was created on each ear. Excision was made by 4 mm biopsy punch (Clark, NY) extending down to bare cartilage, followed by dissection with a microknife (Roboz, MD). Nicks were made on ear cartilage to mark the origin of wound. All the wounds were covered with an occlusive polyurethane dressing (Tegaderm, 3M, Minneapolis, MN until harvest. Upon harvest, animals were euthanized by lethal intraperitoneal injection of ketamine and xylazine. The wounds were bisected and analyzed histologically. These wounds, splinted by underlying cartilage, were minimally Re-epithelialization rate, percentage of full re-epithelialization, and new granulation tissue

formation in all age and sex matched wounds were measured by computer assisted image analysis program Osteomeasure (Osteometrics, Inc. Atlanta, GA).

5 <u>B.</u> Tissue preparation, Histology, and VEGFR1R2-FcΔC1(a) injections were done as described supra in Example 35.

Results

A. Wound healing in K14VEGF transgenic mice

One wound was introduced onto each ear of homozygous K14VEGF transgenic mice. Wounds were harvested on days 3, 7 and 10 after surgery. Cryosections were stained with H&E for morphological analysis. Wound tissue was quantified for granulation tissue formation and neo-epithelialization using a computer-assisted imaging program Osteomeasure (Osteometrics, Inc. Atlanta, GA). In 3 month old K14VEGF transgenic mice, granulation tissue formation was impaired by 37.8% (p<0.05) on POD3 compared to age-matched wild type littermate control mice.



B. The effects of VEGFR1R2-Fc (a) on wound healing in normal mice

As stated *supra*, overexpression of VEGF in mouse skin retards wound healing, presumably due to an excessive inflammatory response and edema. However, in this experiment, blocking endogenous VEGF in normal FVB mouse wounds by administering VEGFR1R2-FcΔC1(a) at 25 mg/kg does not affect wound healing in a significant way. This may be due to the relatively lower levels of VEGF in a "normal" wound as compared to the high levels of expression in chronic wounds which tend not to heal efficiently. Based upon these observation, Applicants contend that VEGFR1R2-FcΔC1(a) will be useful in improving and enhancing wound healing in clinical settings in which VEGF is overexpressed by down regulating inflammation and edema.